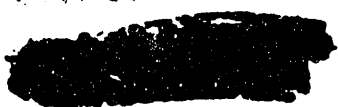


UNCLASSIFIED



CIRCULATING COPY  
RECEIVED 300 AREA  
AUG 27 1956  
RETURN TO  
TECHNICAL INFORMATION FILES

HW-38418

AEC RESEARCH AND DEVELOPMENT REPORT  
TECHNOLOGY - HANFORD PROCESSES -  
REACTOR TECHNOLOGY

COPY No. 40  
C-44a

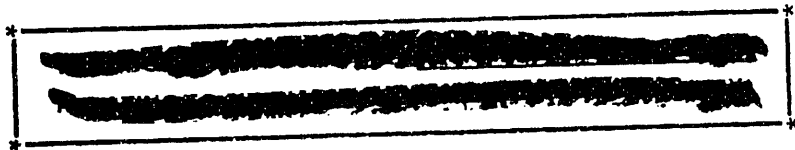
# FINAL REPORT - PT-105-548-A

## THE EFFECT OF MASONITE BURNOUT ON SHIELD ATTENUATION PROPERTIES

BY  
W. L. BUNCH  
PILE TECHNOLOGY SECTION  
ENGINEERING DEPARTMENT

HW--38418  
DE93 008930

MAY 23, 1956



THIS DOCUMENT CONTAINS RESTRICTED DATA AS  
DEFINED IN THE ATOMIC ENERGY ACT OF 1954 AS  
AMENDED BY THE DISPOSITION OF ITS CON-  
TENTS IN ACCORDANCE WITH AN AUTHORIZED  
PERSON IS PROHIBITED

HANFORD ATOMIC PRODUCTS OPERATION  
RICHLAND, WASHINGTON

GENERAL  ELECTRIC

MASTER

DISTRIBUTION RESTRICTED TO U.S. ORNL  
*ep* 

## LEGAL NOTICE

This report was prepared as an account of Government sponsored work. Neither the United States, nor the Commission, nor any person acting on behalf of the Commission:

A. Makes any warranty or representation, express or implied, with respect to the accuracy, completeness, or usefulness of the information contained in this report, or that the use of any information, apparatus, method, or process disclosed in this report may not infringe privately owned rights; or

B. Assumes any liabilities with respect to the use of, or for damages resulting from the use of any information, apparatus, method, or process disclosed in this report.

As used in the above, "person acting on behalf of the Commission" includes any employee or contractor of the Commission to the extent that such employee or contractor prepares, handles or distributes, or provides access to, any information pursuant to his employment or contract with the Commission.

UNCLASSIFIED

HW-38418

**SPECIAL RE-REVIEW  
FINAL DETERMINATION  
DECLASSIFICATION CONFIRMED**

Technology - Hanford Processes -  
Reactor Technology  
(M-3679, 17th Ed.)

BY PL DATE 7-2-81  
BY JW Jordan DATE 7-7-81

This document consists of 52 pages. Copy No. 40  
of 173 copies. Series       

FINAL REPORT - PT-105-548-A  
THE EFFECT OF MASONITE BURNOUT ON  
SHIELD ATTENUATION PROPERTIES

By

W. L. Bunch

Pile Physics Unit  
Pile Engineering Sub-Section

May 23, 1956

CLASSIFICATION CANCELLED

Per LOC 2/11/97  
By L. Pope 5/24/97

OFFICIAL CLASSIFICATION  
OF REPORT IS UNCLASSIFIED  
ALTHOUGH THE NEW CLASSIFICATION  
HAS NOT BEEN ADDED TO ALL PAGES.

HANFORD ATOMIC PRODUCTS OPERATION  
RICHLAND, WASHINGTON

Work performed under Contract #W-31-109-Eng-52 between  
the Atomic Energy Commission and General Electric Company

This document contains Restricted Data as defined in the Atomic Energy Act of 1954. The distribution of its contents in any form to an unauthorized person is prohibited.

Route To:	P. R. No.	Location	Files Route Date	Signature and Date
<u>J. E. Wood</u>	<u>13373</u>	<u>1703D</u>	<u>8-28-56</u>	<u>[Signature]</u>
<u>E. G. Peterson</u>	<u>7761</u>	<u>1709D</u>	<u>[Signature]</u>	<u>[Signature]</u>
<u>H. D. Davis</u>	<u>13084</u>	<u>762</u>	<u>[Signature]</u>	<u>[Signature]</u>

Printed in USA. Charge 45 cents. Available from the U. S. Atomic Energy Commission, Technical Information Extension, P. O. Box 1001, Oak Ridge, Tennessee. Please direct to the same address inquiries covering the procurement of other classified AEC reports.

~~CONFIDENTIAL - SECURITY INFORMATION~~

Technology - Hanford Processes -  
Reactor Technology  
(M-3679, 17th Ed.)

INTERNAL DISTRIBUTION

Copy Number

1	J. T. Baker - R. D. Carter
2	J. W. Baker
3	L. V. Barker
4	R. S. Bell
5	J. A. Berberet - W. E. Fry
6	C. W. Botsford
7	J. H. Brown - R. O. Gumprecht
8	R. O. Brugge - C. L. Miller
9	L. P. Bupp
10	W. L. Bunch
11	A. B. Carson - G. L. Locke
12	R. G. Clough - C. N. Knudsen
13	M. M. Cox
14	R. L. Dickeman
15	J. E. Faulkner - E. D. Clayton
16	E. J. Filip - G. F. Owsley
17	G. C. Fullmer
18	P. F. Gast
19	O. H. Greager
20	R. B. Hall
21	E. T. Hubbard - D. E. Simpson
22	P. C. Jerman
23	C. G. Lewis - F. C. Franklin
24	A. R. Maguire
25	C. A. Mansius
26	L. H. McEwen
27	R. E. McGrath - A. P. Vinther
28	J. H. M. Miller - D. E. Goins
29	J. F. Music - J. W. Sowards
30	J. G. Myers
31	S. L. Nelson - Y. Murakami
32	W. J. Ozeroff - G. W. Stuart
33	R. S. Paul
34	P. H. Reinker
35	W. C. Roesch - J. DePangher
36	O. C. Schroeder
37	H. G. Spencer
38	J. W. Talbott - G. J. Rogers
39	H. T. Wells - W. S. Nechodom
40	D. E. Wood
41	F. W. Woodfield
42	300 Files
43	300 Files - Extra

UNCLASSIFIED

-3-

HW-38418

Technology - Hanford Processes -  
Reactor Technology  
(M-3679, 17th Ed.)

EXTERNAL DISTRIBUTION

Copy Number

44	Argonne National Laboratory, Attn: W. H. Zinn
45	Armed Forces Special Weapons Project, Sandia
46	Armed Forces Special Weapons Project, Washington
47-48	Atomic Energy Commission, Washington
49	Chicago Patent Group
50-53	duPont Company, Aiken
54	duPont Company, Wilmington
55	Hanford Operations Office
56	Hanford Operations Office, Attn: J. M. Musser and H. H. Schipper
57	Patent Branch, Washington
58	Union Carbide Nuclear Company (ORNL) Attn: A. M. Weinberg
59-173	Technical Information Service, Oak Ridge



TABLE OF CONTENTS

	<u>Page</u>
INTRODUCTION . . . . .	7
SUMMARY . . . . .	7
DISCUSSION . . . . .	8
A. Experimental Procedure . . . . .	8
B. Interpretation of Data . . . . .	21
C. Sources of Error . . . . .	27
1. Lucite Integrator . . . . .	27
2. Sulfur Foils . . . . .	30
3. Residue Composition . . . . .	31
4. Capture Gamma Flux . . . . .	33
5. Temperature Distribution . . . . .	34
6. Facility Edge Effects . . . . .	34
D. Conclusions . . . . .	35
ACKNOWLEDGMENTS . . . . .	36
REFERENCES . . . . .	37
APPENDIX . . . . .	38



LIST OF FIGURES

<u>Figure</u>		<u>Page</u>
1	Masonite Removal - Disassembled Test Slab . . . . .	10
2	Masonite Removal - Assembled Test Slab . . . . .	11
3	Neutron Attenuation Data, Configuration 0 . . . . .	12
4	Neutron Attenuation Data, Configuration 1 . . . . .	13
5	Neutron Attenuation Data, Configuration 2 . . . . .	14
6	Neutron Attenuation Data, Configuration 3 . . . . .	15
7	Neutron Attenuation Data, Configuration 4 . . . . .	16
8	Neutron Attenuation Data, Configuration 3A . . . . .	17
9	Neutron Attenuation Data, Configuration 4A . . . . .	18
10	Lucite Integrator and Gamma Chamber . . . . .	19
11	Cave to Minimize Backscatter . . . . .	22
12	Loading Thermocouples and Foils into Slabs . . . . .	23
13	Gamma Leakage Data . . . . .	24
14	Temperature Distribution Through Biological Shield . . . . .	25

LIST OF TABLES

<u>Table</u>		<u>Page</u>
I	Attenuation Slab Compositions . . . . .	20
II	Dose Leakage Through Simulated Burned Out Shields . . . . .	28
III	Paraffin Integrator Calibration . . . . .	29
IV	Calculated Attenuation Coefficients . . . . .	32
V	Foil Activation Data, Configuration 1 . . . . .	39
VI	Foil Activation Data, Configuration 2 . . . . .	41
VII	Foil Activation Data, Configuration 3 . . . . .	43
VIII	Foil Activation Data, Configuration 4 . . . . .	45
IX	Foil Activation Data, Configuration 3A . . . . .	47
X	Foil Activation Data, Configuration 4A . . . . .	49
XI	Foil Activation Data, Integrator Summary . . . . .	51



FINAL REPORT - PT-105-548-A  
THE EFFECT OF MASONITE BURNOUT ON  
SHIELD ATTENUATION PROPERTIES


INTRODUCTION

In a previous study it was determined experimentally that heat deterioration, or burnout, of the shield masonite is more severe than radiation damage under existing and proposed operating conditions. Higher shield temperatures, which are expected to result from increased power levels, fringe enrichment, and higher graphite temperatures, will markedly increase the rate at which the masonite burns out. The laminated iron-masonite biological shield will lose, as a result of burnout, the hydrogen and oxygen necessary to attenuate and moderate neutrons.

The purpose of this production test has been to obtain experimental data from which future shield leakage rates could be estimated. The attenuation data reported here were obtained in the DR pile bulk shield facility from experiments using various void spacings to simulate burnout conditions. From these data it was hoped to determine (1) the resultant attenuation properties of the shields, and (2) the exposure rates due to radiation penetrating the shield.

SUMMARY

Flux measurements taken in this test through shield iron-masonite configurations corresponding to predicted burnout conditions indicate that eventual burnout is expected to result in dose rates equivalent to several roentgens per hour (see Table II); the resultant dose rate will consist primarily of intermediate energy neutrons. These data have already been used in conjunction with data from masonite burnout rate experiments to



estimate radiation leakage through imperforate shields as a function of time and pile operating history. <sup>(1, 2)</sup> It appears likely that radiation leakage will severely limit access to the experimental levels and top of the unit of the B, D, F, DR, and H piles within one to two years of operation after the completion of the current water plant expansion project unless preventive action is taken. For this reason companion studies are underway to develop measures to minimize burnout by the use of fringe poisoning, <sup>(3)</sup> to compensate excess shield leakage by exterior shield patches, <sup>(4)</sup> and to measure the neutron spectrum more exactly to permit "living with" anticipated burnout conditions. Test results indicate that one of the above approaches, or a combination of them, will preclude serious limitations to pile life and operating efficiency due to shield radiation leakage. Mechanical failure of the shield as a possible result of masonite deterioration <sup>(5)</sup> has not been considered in this report.

## DISCUSSION

### A. Experimental Procedure

The attenuation measurements were made in one of the two wells of the bulk shield facility located on the top of the DR pile. Each of these facilities consists of a lined opening which increases in five steps from about three feet square at the bottom to three and a half feet square at the outside of the shield. The bottom liner of the well is in contact with the

- 
- (1) HW-38419, "Iron-Masonite Shield Effectiveness as a Function of Pile Operating Conditions", L. A. Wilson, 1-19-55 (Secret).
  - (2) HW-35202, "Hanford Shield Shield Masonite Deterioration Studies", L. A. Wilson, 8-8-55 (Secret).
  - (3) HW-40997, "Interim Report - PT-105-604-A - Reducing Side Shield Temperature by Fringe Poisoning", W. L. Bunch, 1-19-55 (Secret).
  - (4) HW-41189, "FY 1958 Budget Study, Shield Patches, B, D, F, DR, and H Reactors", C. A. Mansius, 2-1-56, (Official Use Only).
  - (5) HW-41507, "Possible Mechanical Effects of Extreme Masonite Deterioration in Laminated Biological Shields", G. J. Rogers, 3-22-56 (SECRET).

T-section flanges of the biological shield; the facility thus penetrates through the four foot laminated structure of the biological shield and is separated from the active region of the pile by ten inches of iron and the two foot graphite reflector. A set of attenuation slabs composed of iron and masonite laminations matching the regular biological shield structure had been built and used in a previous study.<sup>(6)</sup> These slabs were altered for the present test by simply removing sheets of masonite from each layer while maintaining the laminar spacing with steel washers placed at the corner of the slabs. This procedure is illustrated in Figures 1 and 2. A total of six different burnout configurations were used during the test; these are given in Table I and are pictorially illustrated in Figures 3 - 9 which also summarize the neutron foil activation data.

The neutron measurements were made using the same foil techniques employed previously.<sup>(6)</sup> This procedure consists of activating three types of foils which are each sensitive to a limited interval of the incident neutron energy spectrum. The three foils are: (1) bare gold foils which are activated by both thermal and resonance (predominantly 5 ev) neutrons, (2) cadmium covered gold foils which are activated primarily by resonance energy neutrons, and (3) cadmium covered sulfur foils which are activated by an (n, p) reaction which has a threshold at about 1 Mev and hence detect only high energy neutrons. This method of detection leaves a great deal of the neutron energy spectrum unmonitored, but under certain conditions it does provide sufficient data for attenuation analysis.

To obtain more information about the neutron flux penetrating the burned out mockups and to be able to better estimate leakage dose rates, a "lucite integrator" was placed on top of the test well. The lucite integrator consisted of one foot square lucite (methyl methacrylate) plates stacked with gold foils between the sheets until an approximate one foot cube was formed as in Figure 10. The foils were placed in a helical pattern to minimize flux perturbation interaction caused by the absorbing foils.

---

(6) HW-36370, "Attenuation Properties of Hanford Pile Shield Materials", W. L. Bunch and R. L. Tomlinson, 9-1-55 (Secret).

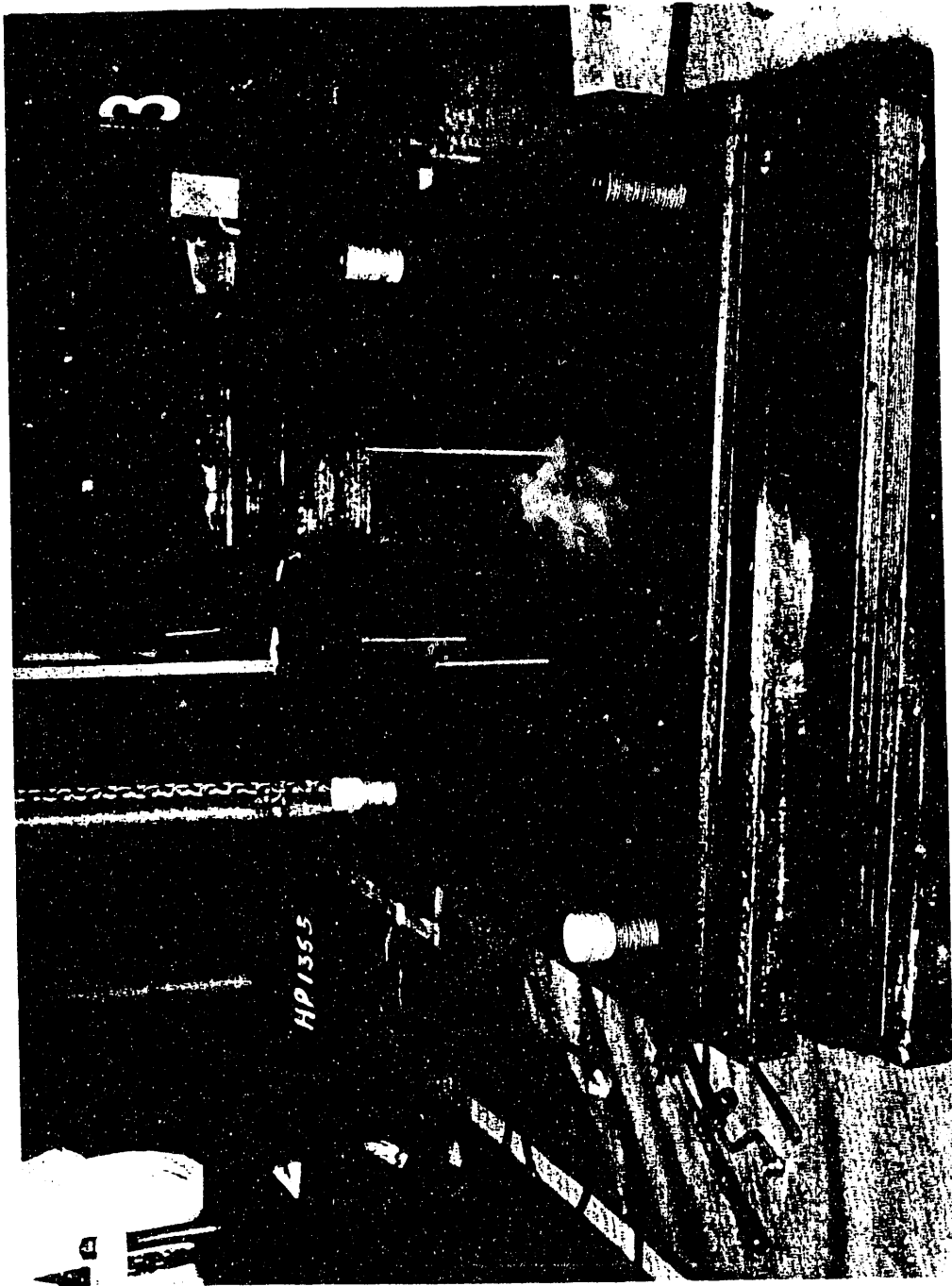


FIGURE 1

Disassembled Test Slab Showing Spacers and Small Amount of Masonite

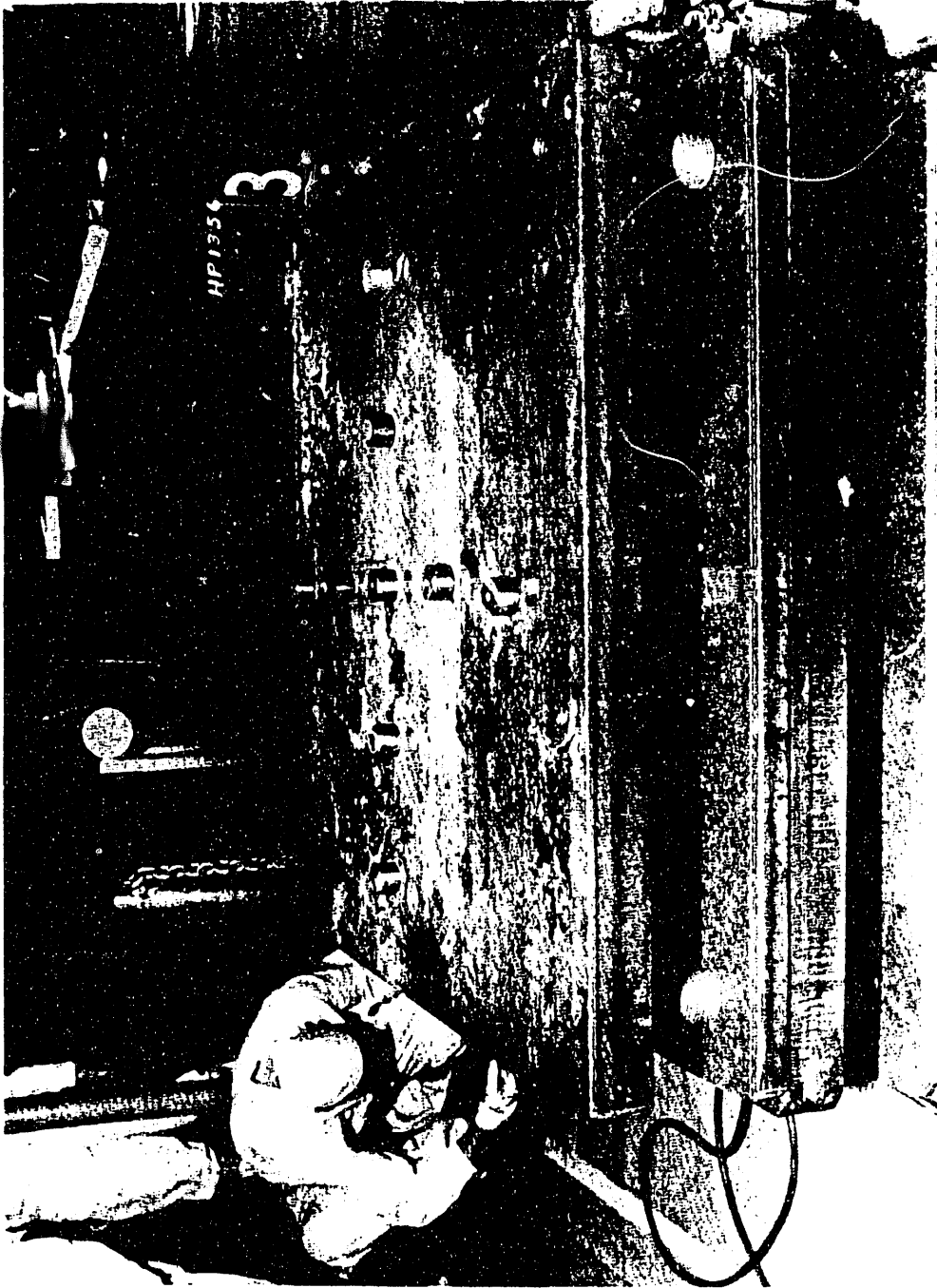


FIGURE 2

Assembled Test Slabs Showing Spacers and Openings for Placement of Foil Detectors

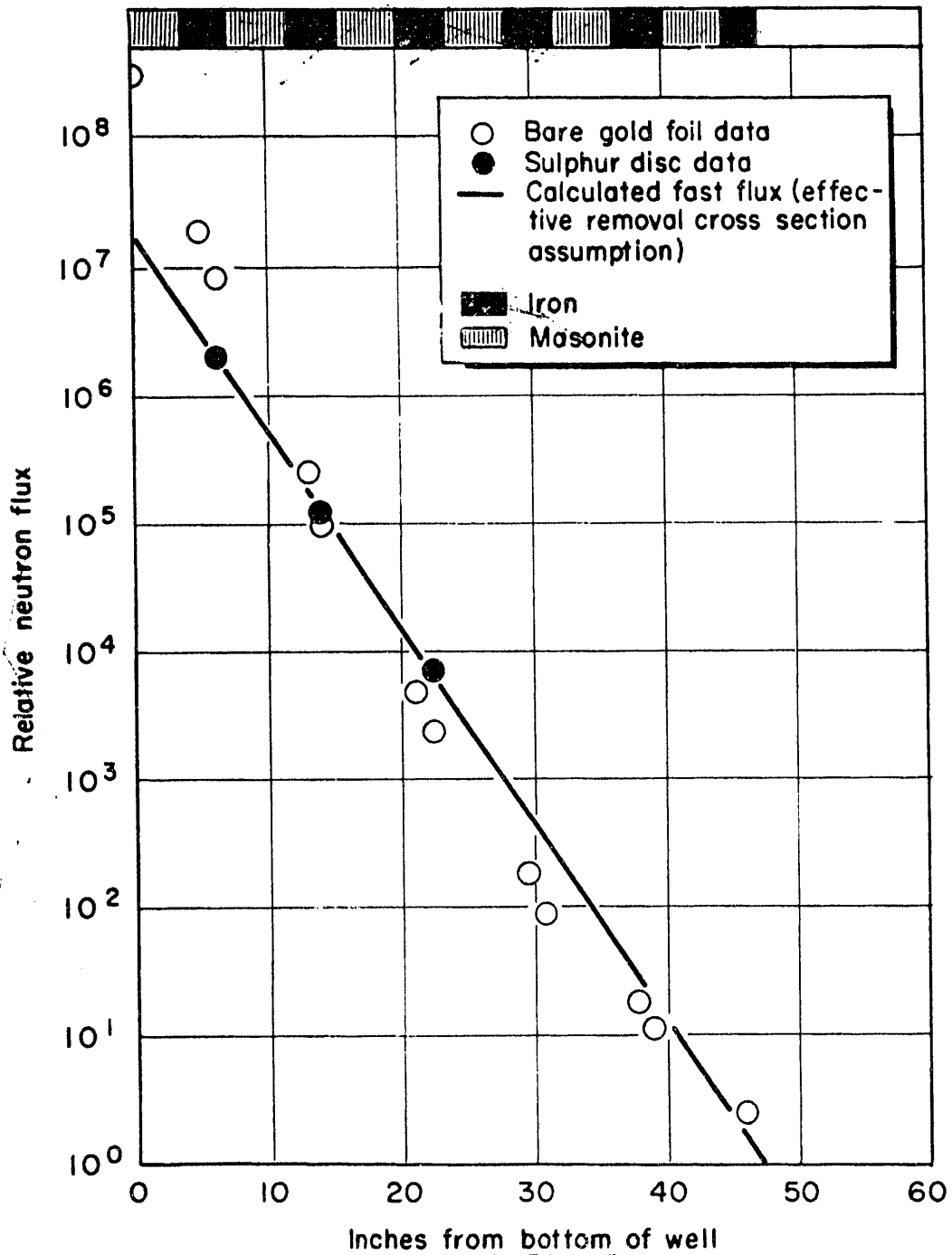
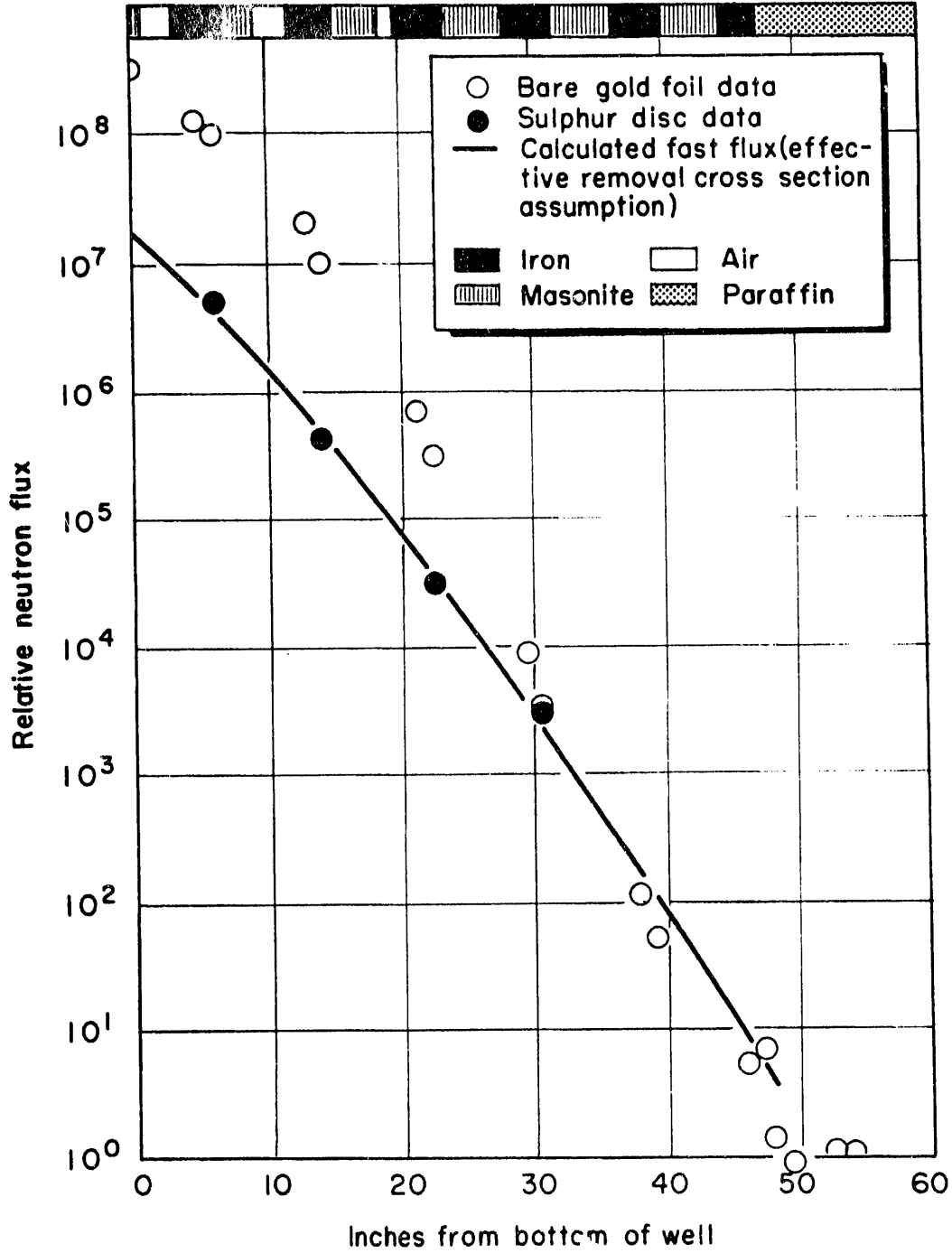
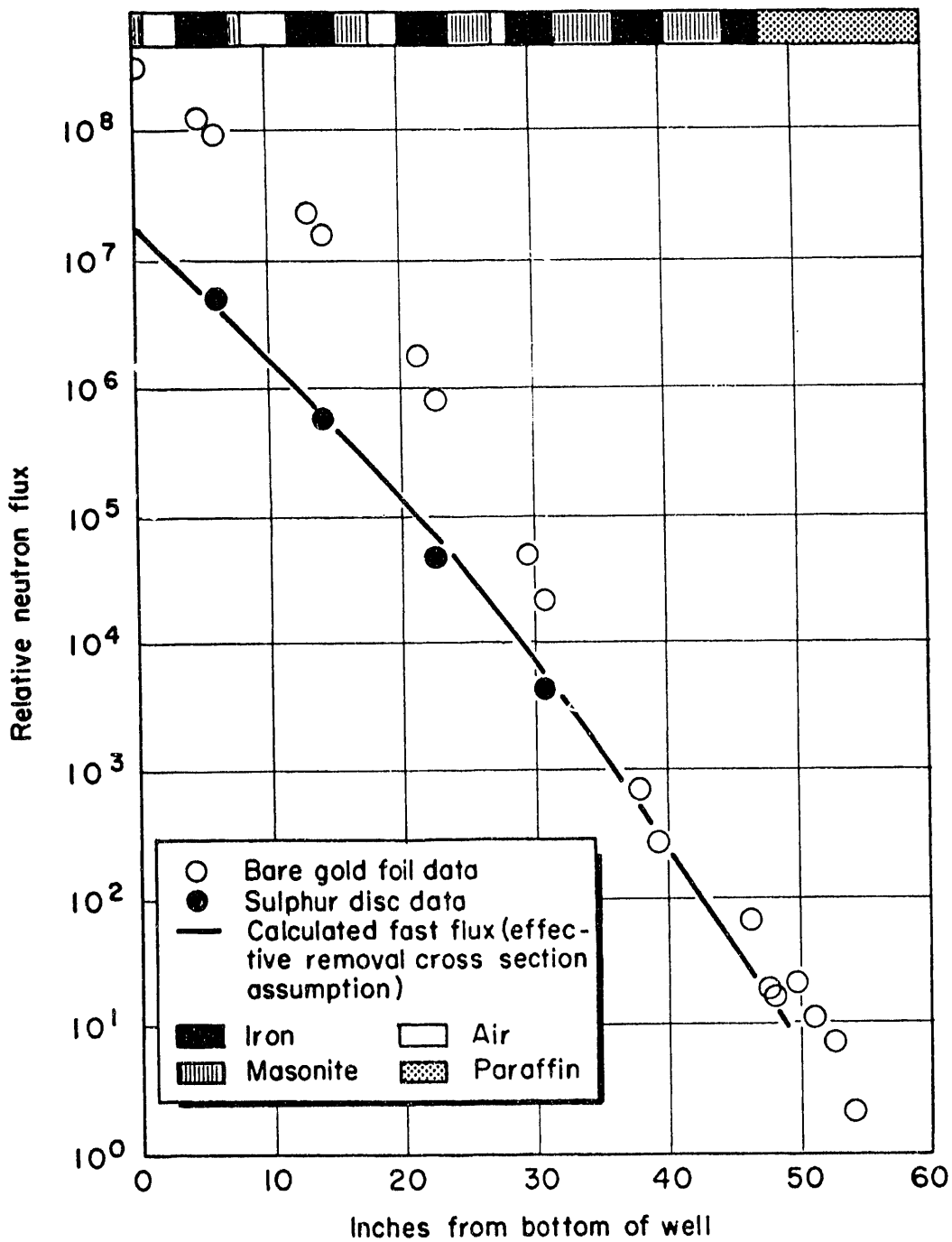
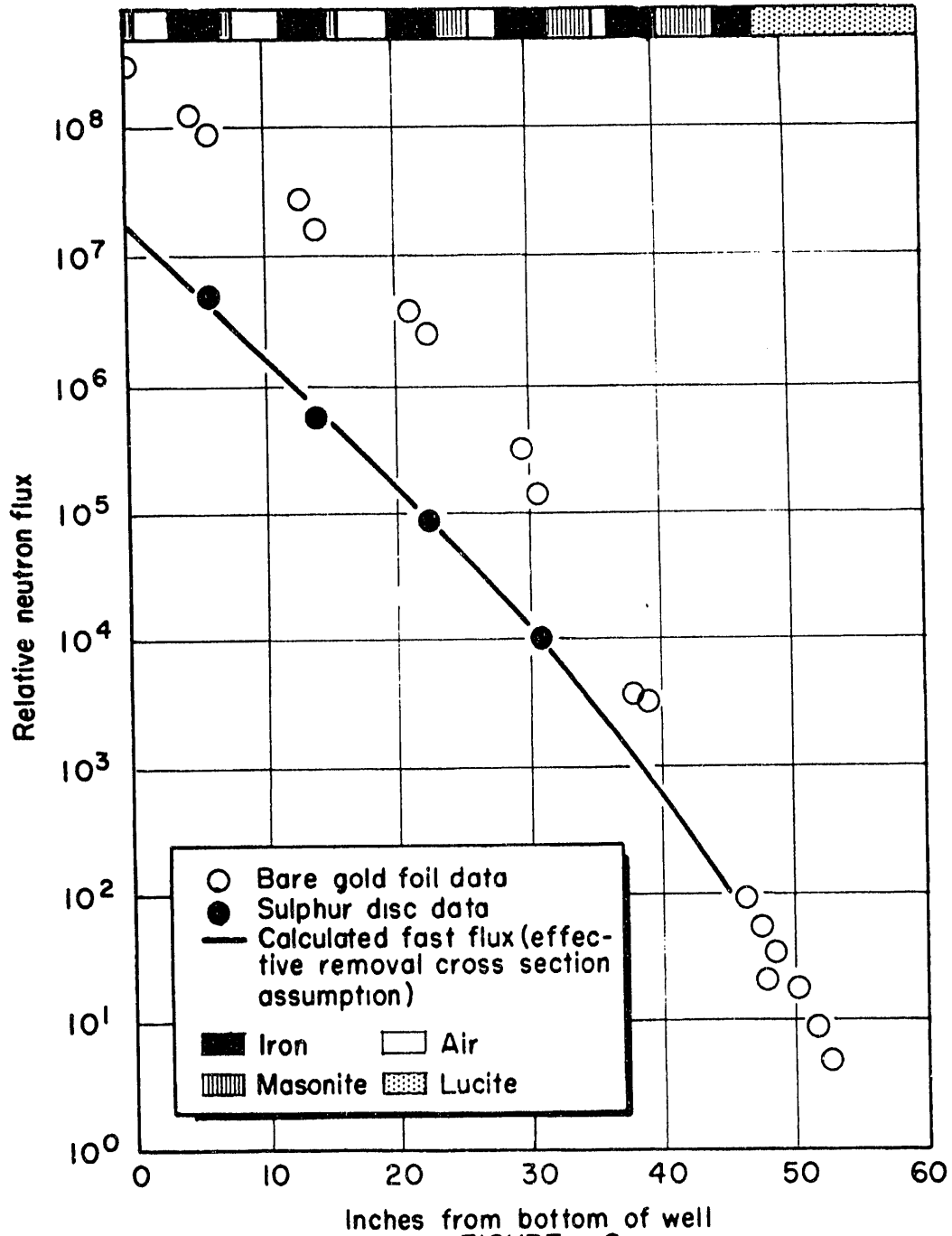


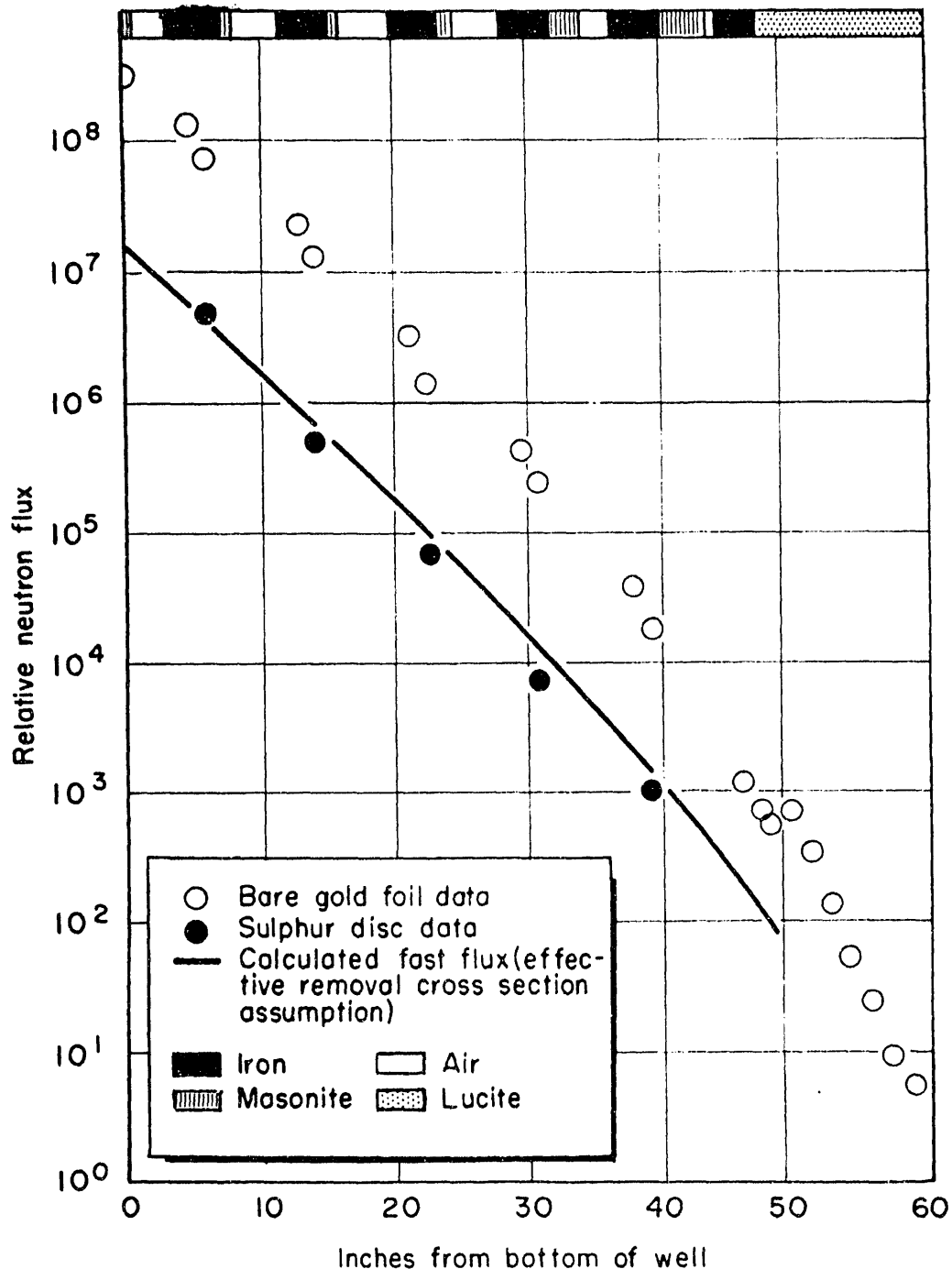
FIGURE 3  
RELATIVE NEUTRON FLUX AS A FUNCTION OF PENETRATION THROUGH A BURNED OUT SHIELD CONFIGURATION 0

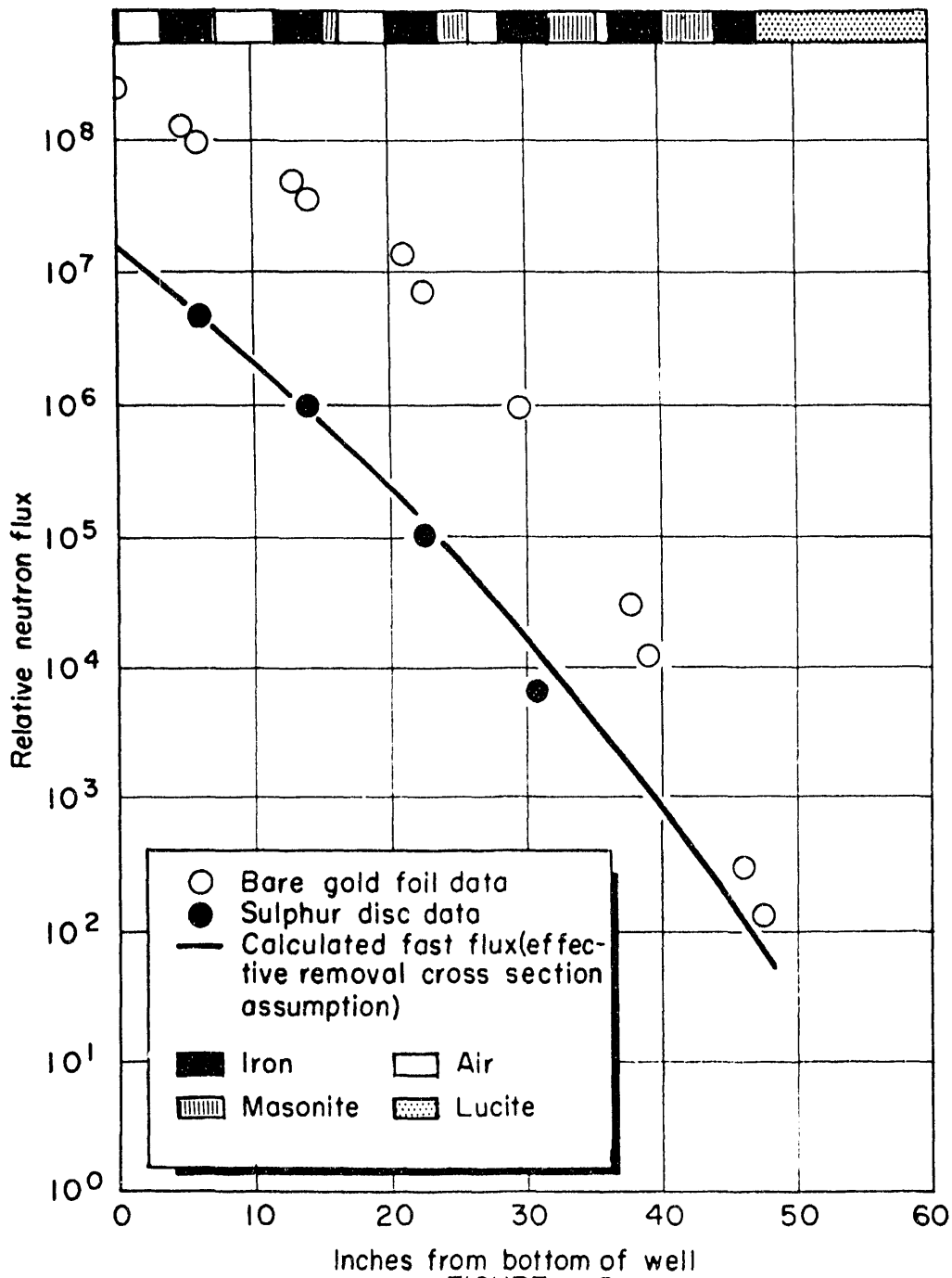


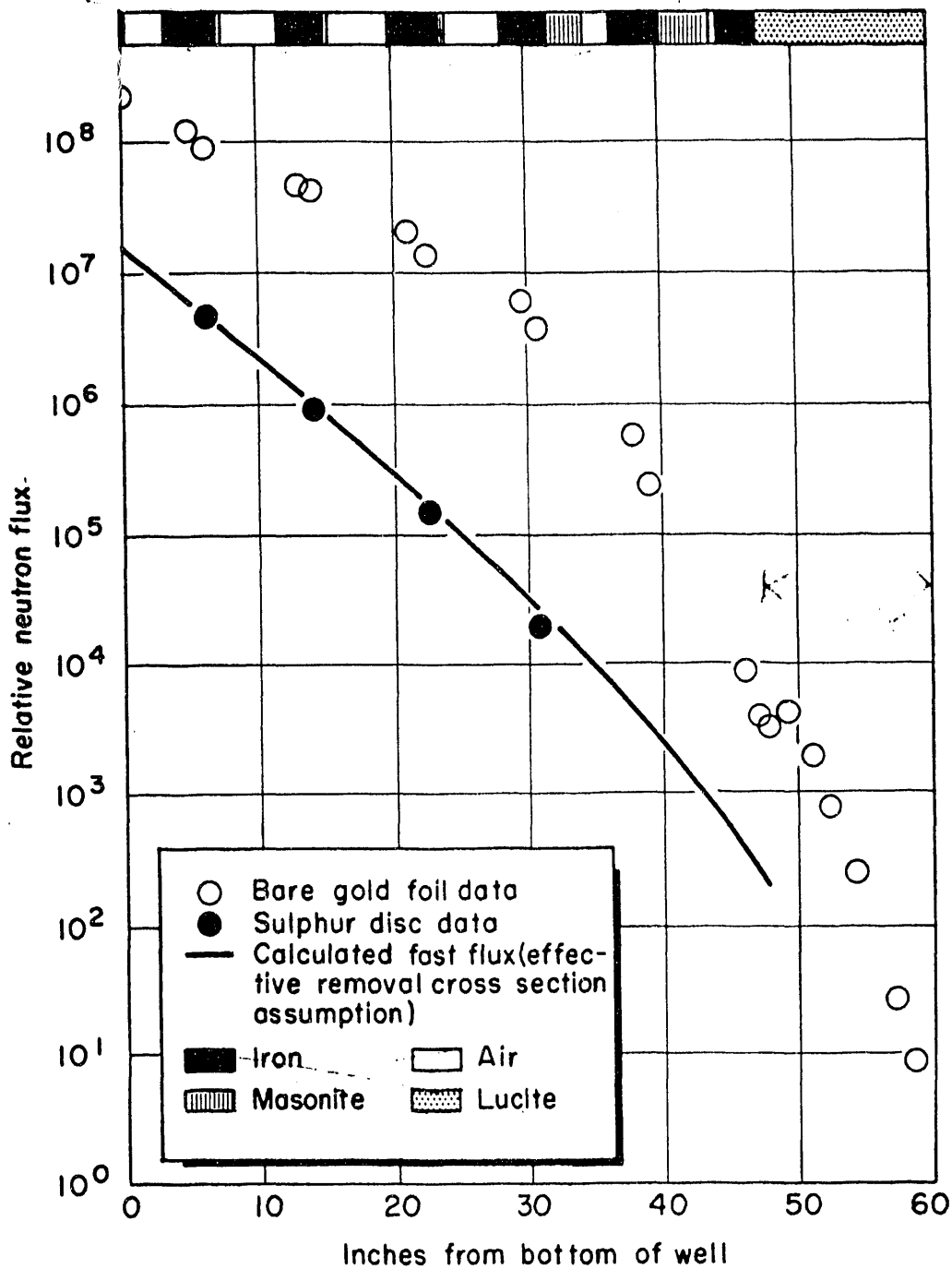












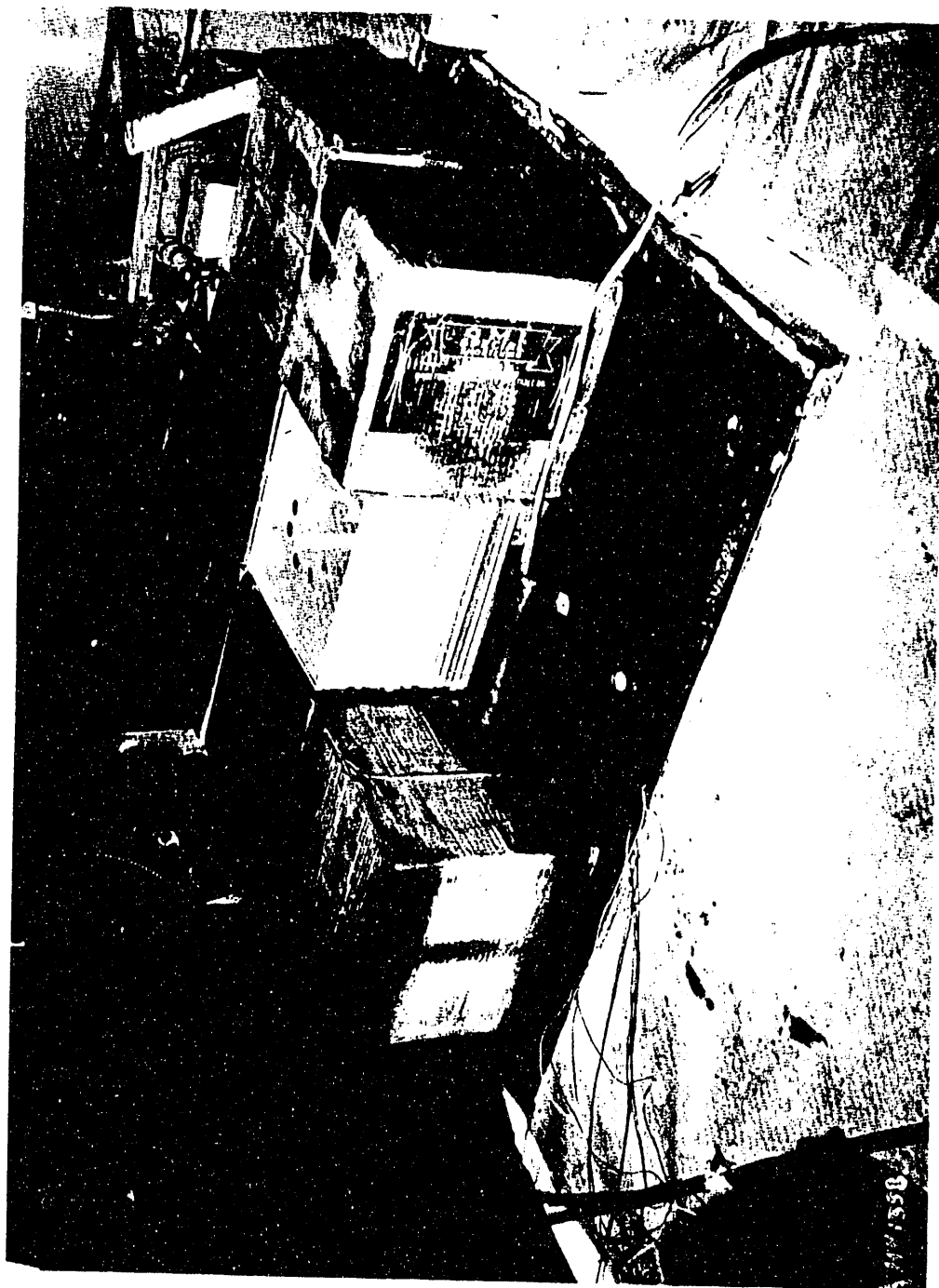


FIGURE 10

Lucite Integrator and 1000 cc Chamber Placed on Top of Well

TABLE I

Simulated Burned-Out Iron-Masonite Attenuation Slab Compositions -  
Inches of Material per Layer in Test Configurations

Layer Number	Material	Configuration Number						
		0	1	2	3	4	3A	4A
1 (inner)	Masonite	3.5	0.9	0.9	0.9	0.9	0.1	0.1
	Iron	3.75	3.75	3.75	3.75	3.75	3.75	3.75
2	Masonite	4.5	2.3	1.1	1.1	1.1	0.3	0.3
	Iron	3.75	3.75	3.75	3.75	3.75	3.75	3.75
3	Masonite	4.5	3.4	2.3	1.1	1.1	1.3	0.3
	Iron	3.75	3.75	3.75	3.75	3.75	3.75	3.75
4	Masonite	4.5	4.5	3.4	2.3	1.1	2.4	0.8
	Iron	3.75	3.75	3.75	3.75	3.75	3.75	3.75
5	Masonite	4.5	4.5	4.5	3.4	2.3	3.5	2.4
	Iron	3.75	3.75	3.75	3.75	3.75	3.75	3.75
6 (outer)	Masonite	4.5	4.5	4.5	4.5	3.4	4.3	4.0
	Iron	2.50	2.50	2.50	2.50	2.50	2.50	2.50
Inches of Masonite removed		0	6	9.4	12.75	16.1	14.25	18.1
% of total Masonite removed		0	23	36	49	62	55	70

The purpose of an integrator is to thermalize the entering neutrons thereby simplifying the problem of detecting them. Utilizing the flux distribution within the integrator, a crude estimate can be made of both the number and "effective energy" of the incident neutrons.

The gamma intensity penetrating the burned out shield section was measured with a 1000 cc ionization chamber which had been calibrated and used for the previous attenuation measurements. <sup>(6)</sup> The chamber was used only outside the well and was placed alongside the lucite integrator as shown in Figure 10. Because of the leakage of neutrons and gamma radiation around the VSR openings, the background radiation on top of the unit is rather high. Boxes of borated paraffin were placed around the integrator and chamber, and a top covering consisting of a paraffin slab and lead bricks was used to protect the measurements from this perturbing effect. This arrangement is shown in Figure 11.

Iron-constantan thermocouple junctions were located at the center of each slab by placing the leads in grooves cut in the masonite strips used to hold the foils. The leads were brought out of the well to a switch-box (see Figure 12), where the several thermocouples could be read rapidly and accurately with a Rubicon potentiometer. Standard tables were used for converting each emf reading to a delta temperature above ambient.

#### B. Interpretation of Data

An abridged version of the neutron data obtained during this test is tabulated in the Appendix, and Figures 3 - 9 epitomize the data. The gamma attenuation data are presented in Figure 13. A typical "equilibrium" temperature traverse is shown in Figure 14.

A primary goal of the measurements has been to determine the dose rate penetrating the shield as a function of burnout. The gamma data were obtained directly in terms of mrem/hour, but it was necessary to approximate neutron leakage dose rates from the foil measurements.

---

(6) Op. Cit.

[REDACTED]

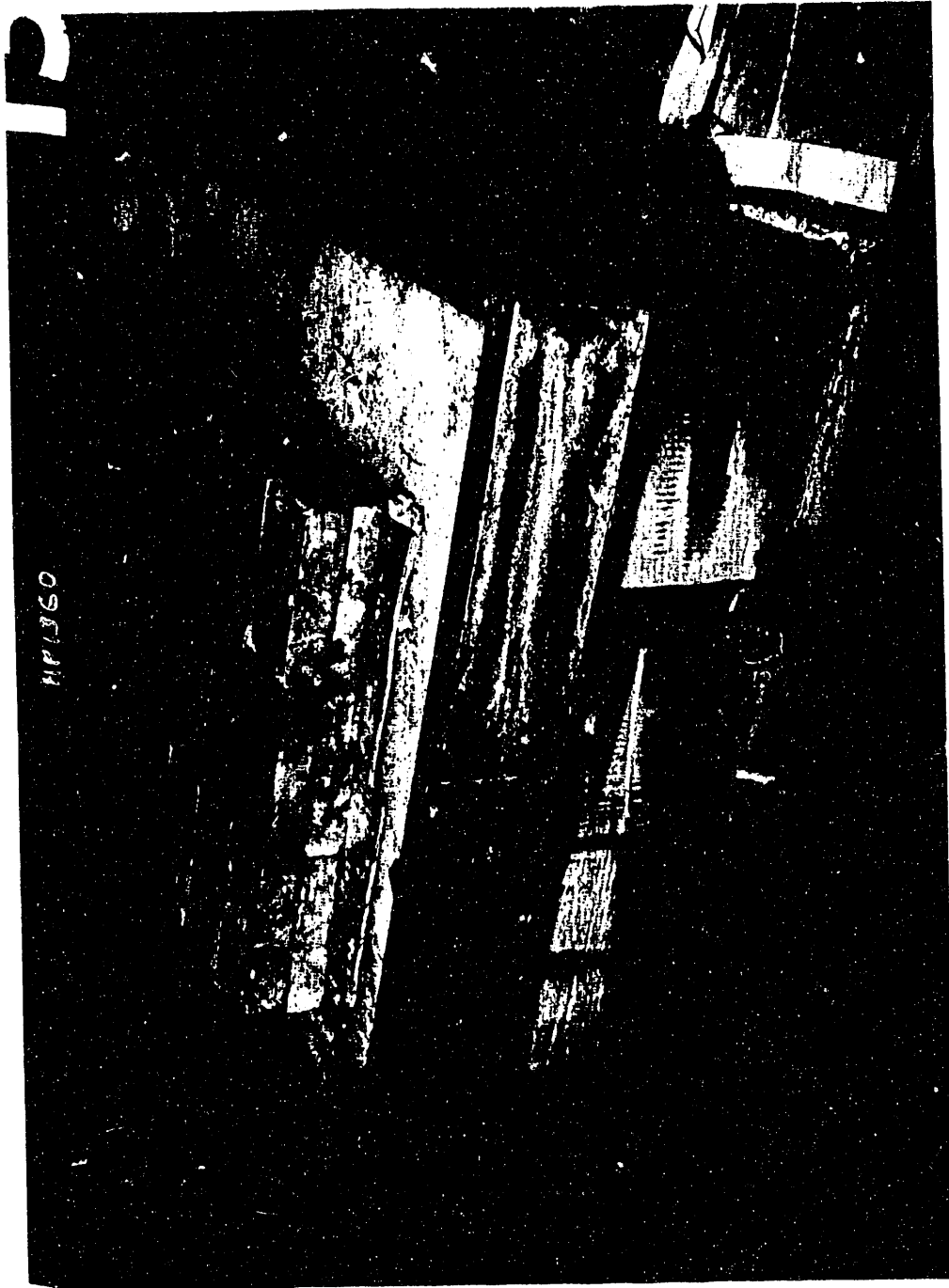


FIGURE II

Lead and Paraffin Cave to Prevent Backscatter into Assembly



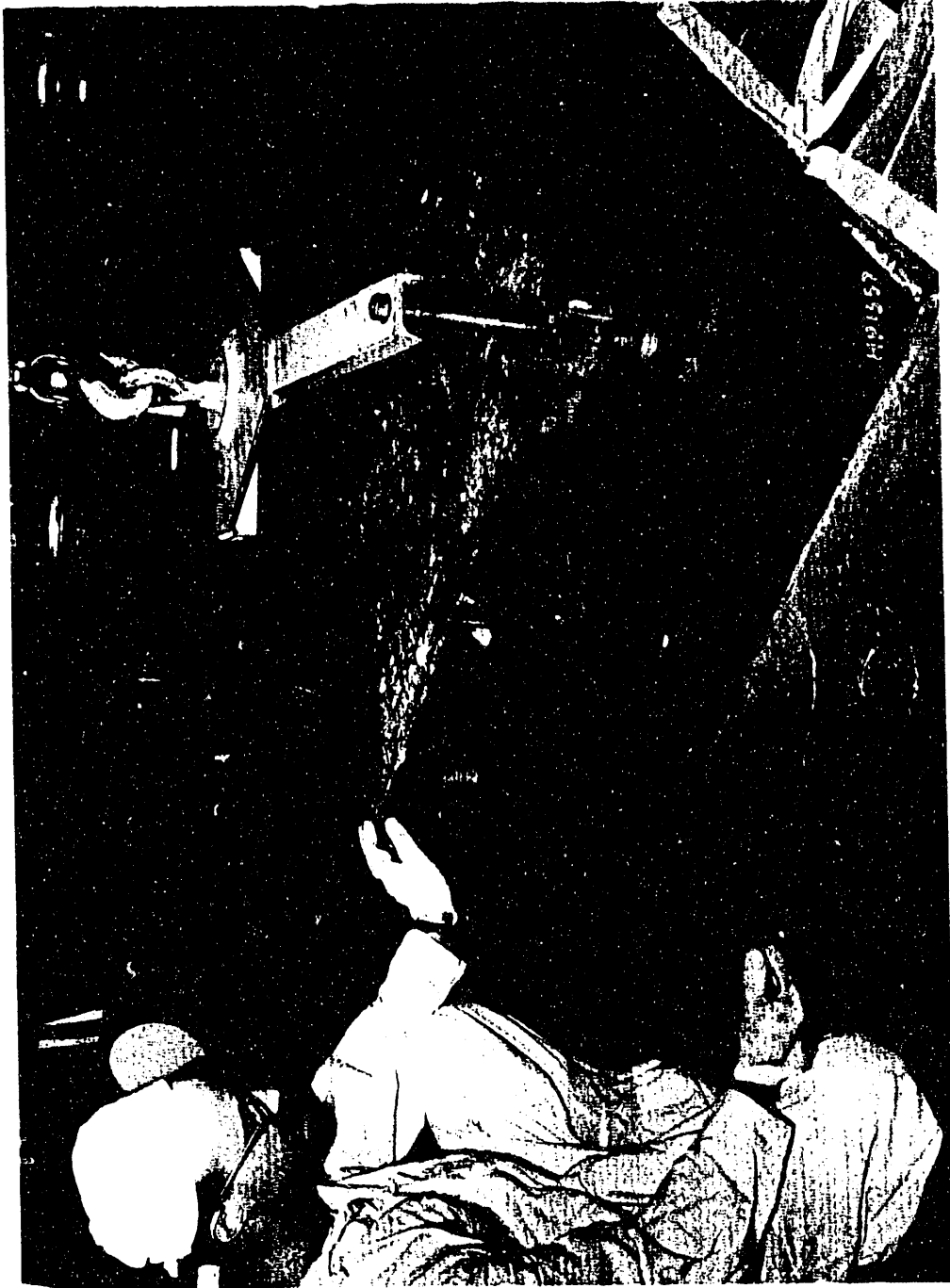


FIGURE 12

Placement of Thermocouple and Foils into Test Slab

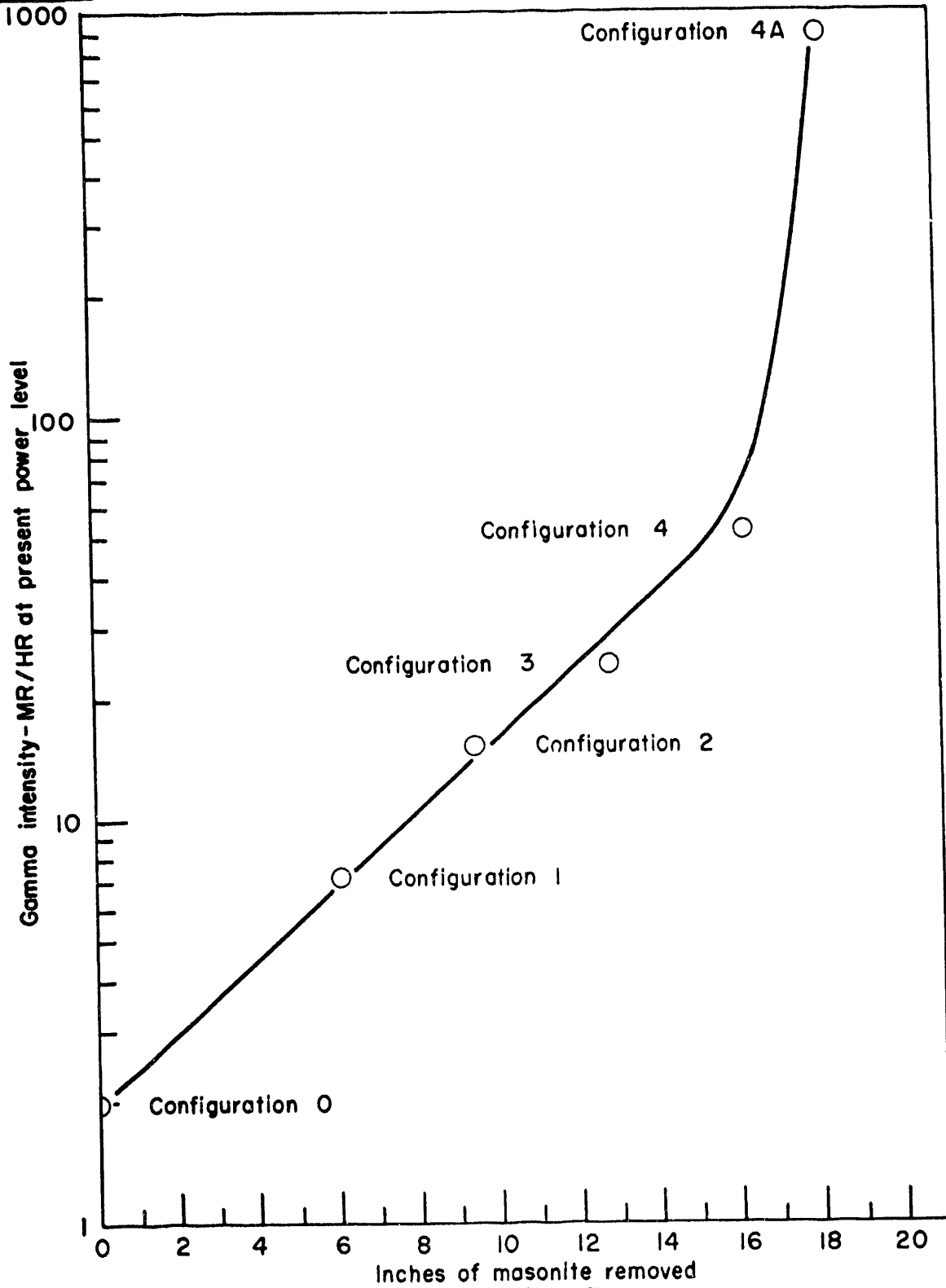


FIGURE 13  
GAMMA INTENSITY THROUGH SHIELD CONFIGURATIONS AS A FUNCTION OF MASONITE REMOVAL

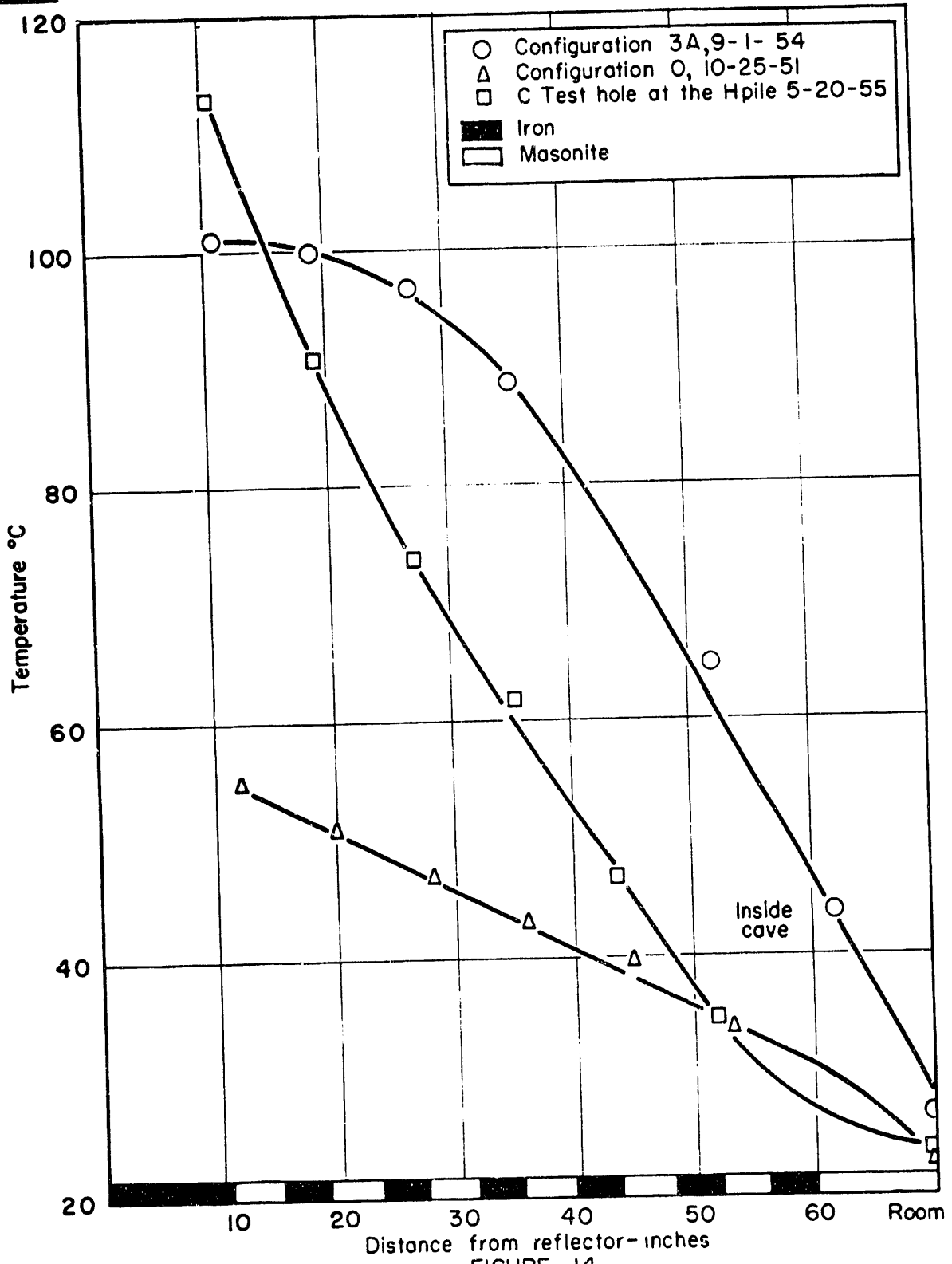


FIGURE 14  
TEMPERATURE DISTRIBUTION THROUGH BIOLOGICAL SHIELD

Thermal neutron flux intensity has been estimated from the bare and cadmium covered gold foil activity. These foils have been calibrated in the Hanford Standard Pile (radium-beryllium source in a graphite stack) where the thermal flux is known.<sup>(7)</sup> A conversion factor of  $100 \text{ n/cm}^2 \text{ sec per mrem/hr}$  was used for the thermal flux.

Fast neutron dose rates were approximated by extrapolating the available sulfur foil data to the surface of the shield using the effective removal cross sections obtained previously.<sup>(6)</sup> Sulfur foil activity has been "calibrated" in terms of neutron flux by normalization to a theoretical neutron flux distribution within the active region of the pile.<sup>(2, 6, 8, 9, 10)</sup> The fast neutron flux has been converted to dose rate by assuming an average value of  $5 \text{ n/cm}^2 \text{ sec per mrem/hr}$ .

Intermediate energy neutron dose rates have been estimated from the lucite integrator data. The distribution of thermal neutrons within the integrator indicates that the average effective energy of leakage neutrons is less than 0.1 Mev. A conservative conversion factor of  $25 \text{ n/cm}^2 \text{ sec per mrem/hr}$  has been used for this intermediate energy flux.

- 
- (7) HW-26207, "The Standardization of Gold and Indium Foils and the Absolute Neutron Flux Determination in the Hanford Standard Pile", D. E. Davenport, G. L. Lynn, and C. R. Richey, 8-27-54, (Declassified).
  - (8) HW-29125, "Measurement of Neutron Fluxes in Graphite Reflector", R. L. Tomlinson, 9-1-53 (Secret).
  - (9) HW-29135, "Measurement of Neutron Flux Spectra Inside Reactors", R. E. Heineman, 8-26-53 (Secret).
  - (10) HW-28303, "Neutron Energy Spectra in a Hanford Pile", R. E. Heineman and J. W. Culvahouse, 6-5-53 (Secret).

A total of six different burnout conditions have been mocked up in the measurements. Two different assumptions were made in the removal of the masonite so that two different sets of burnout conditions are approximated. In the first series of tests, numbered 1, 2, 3 and 4, it was assumed that (1) a linear temperature distribution exists through the shield, and (2) the ultimate residue may be approximated by one-fourth of the original masonite. As the testing progressed these assumptions did not appear to be conservatively realistic, and condition 3A and 4A were mocked up. In the latter tests, it was assumed that (1) burnout of succeeding layers is enhanced by the burnout of the previous layer, and (2) the calculated shielding effectiveness of the final residue is more realistically approximated by about one-twentieth of the original masonite. The leakage for the various conditions estimated from test data is shown in Table II.

### C. Sources of Error

There are several factors which limit the accuracy of the interpretation which can be made with these data. Each of these is discussed separately in what is thought to be descending order of importance.

#### 1. Lucite Integrator

The interpretation of the lucite integrator data in terms of neutron dose rate introduces a great deal of uncertainty into the total leakage dose. It is well known that the energy distribution of neutrons is very important in determining dose rate<sup>(11)</sup> and it is also well known that the measurement of a neutron energy spectrum is very difficult. The lucite integrator offered a readily available and inexpensive method of evaluation but one which lacks the resolution necessary for accurate interpretation.

---

(11) RH-1 Reactor Handbook, Volume 1, June 1955, page 946 (Secret).




TABLE II

Radiation Leakage Through Simulated Burned Out Shields

$\phi = n/cm^2 \text{ sec}$

$I \approx mrem/hr$

Configuration	0		1		2		3		4		3A		4A	
	$\phi$	I	$\phi$	I	$\phi$	I	$\phi$	I	$\phi$	I	$\phi$	I	$\phi$	I
Fast	0.7	0.14	4	0.8	11	2.2	30	6	80	16	45	9	170	34
Intermediate	7*	0.28	35*	1.4	210	8.4	500	20	14000	560	---	---	100000	4000
Thermal	2*	0.02	14	0.14	56	.56	280	2.8	3800	38	660	6.6	21000	210
Gamma	---	1.4	---	4.9	---	10	---	18	---	36	---	---	---	630
Total***	---	1.8	---	7.2	---	21	---	47	---	650	---	400**	---	4900

\* Probable upper limit, flux below sensitivity of detection methods employed.

\*\* Data incomplete, total leakage estimated.

\*\*\* Total leakage rate is normalized to the maximum value for fringe tubes operating at 100KW/tube.

The principle of operation of a lucite integrator is that a mono-energetic source of neutrons incident on an hydrogenous medium will be scattered and slowed down to thermal energy. The thermal neutron population will become a maximum at a depth of penetration which is characteristic of the incident neutron energy; for a higher energy mono-energetic source of neutrons this maximum will appear after a deeper penetration since more collisions are required on the average to thermalize the higher energy neutrons. Calibration work of this nature has been reported for bare indium foils in paraffin<sup>(12)</sup> and is summarized in Table III.

TABLE III  
PARAFFIN INTEGRATOR CALIBRATION<sup>(12)</sup>

<u>Neutron Energy</u>	<u>Position of Maximum</u>
0.03 ev	0.3 inches
24 kev	1.0 inches
700 kev	2.1 inches
4.1 Mev	3.0 inches
15 Mev	4.5 inches

Paraffin was used as the integrator in the first two burnout stages but was found to flow because of the high temperatures which existed on top of the experimental well. Lucite was used as a substitute on the basis that the hydrogen content was quite similar to that of paraffin and therefore both should exhibit approximately the same slowing down power for neutrons. The hydrogen contents were calculated using the formula  $C_5H_8O_2$  for lucite and  $C_{25}H_{52}$  for paraffin and assuming densities of 1.2 and 0.8 respectively. These assumptions yield a hydrogen content of  $6 \times 10^{22}$  H/cc for lucite and  $7 \times 10^{22}$  H/cc for paraffin. This was considered to be close enough agreement to permit the use of the table above for

---

(12) BNL-351, "Neutron Monitoring with Indium Foils", F. B. Oleson, July 1955.

estimating the average effective energy of the neutrons which were slowed down in the lucite integrator. In every case the maximum foil activation was attained after approximately one inch penetration into the integrator, which corresponds to a neutron energy of 24 kev. This energy incidentally corresponds to a "window" in the total cross section of iron,<sup>(13,14)</sup> but the energy resolution of the integrator is so poor that the measurement actually indicates only an energy of this order of magnitude rather than determining a specific energy.

A second method of utilizing a lucite integrator to determine effective neutron energy is possible if sufficient calibration work could be done. This method would determine the exponential rate of decrease in the number of neutrons in a particular energy group (such as the 5 ev group measured by a cadmium covered gold foil). However, the cadmium covered data which were obtained were of such low count rate that very little statistical confidence could be placed in the information obtained from it and the method has not been pursued.

## 2. Sulfur Foils

The interpretation of sulfur foil activation in terms of neutron dose rate has been discussed previously.<sup>(6)</sup> The important assumption made in this case is that the high energy spectrum (neutron energy greater than about 1 Mev) does not change appreciably in penetrating the shield. Because of the inelastic scattering cross section in iron, which becomes important at energies greater than 1 Mev, hardening of the neutron energy spectrum should not occur. Buildup in the energy range just below 1 Mev should be detected by the lucite integrator if it exists to any great extent.

---

(13) Physical Review, Volume 85, No. 4, February 15, 1952, "Neutron Transmission Cross Sections in the Kilovolt Region", Carl T. Hibdon, Alexander Langsdorf, Jr., and Robert E. Holland.

(14) Personal Communication, Henry W. Newson. To be published in Physical Review, Volume 102, No. 6, June 15, 1956.

(6) Op. Cit.



Because the integrator did not indicate significant buildup of this energy component, the effluent high energy neutron dose rate has been determined by extrapolating the sulfur foil measurements to the outside of the shield. This extrapolation necessitates the use of "effective removal cross sections", an empirical method for predicting attenuation properties of a given material as a function of its composition.<sup>(6)</sup> Another limitation on the experiment is also introduced; namely, the use of masonite for the residue of the burnout process.

### 3. Residue Composition

A tar-like fluid is formed during the heating of masonite when the oxygen and hydrogen components are evolved. In order to avoid the difficulties involved and to eliminate the delay necessary to actually bake the huge quantities of masonite to the desired state of deterioration, it was deemed expeditious to approximate this situation by simply removing fractional amounts of the masonite. In doing this it becomes necessary to determine the relationship which exists between masonite and the expected residue. The effective removal cross sections determined previously were used for calculating fast neutron attenuation coefficients; the photon cross sections were based on a 6 Mev photon energy from the results of the previous study.<sup>(6)</sup> The cases which have been calculated are (1) the anticipated residue, which is thought to consist of 30% of the carbon contained in the masonite, and (2) a 5/16" thick layer of masonite, which was the residue left in the test to approximate the ultimate burnout condition. The calculations are summarized in Table IV. The composition of the thin masonite layer used to simulate ultimate burnout conditions does not duplicate the final expected composition. However, it can be seen that resultant fast neutron and gamma attenuation coefficients are within 2% of the expected coefficients and this is less than the experimental error involved in making attenuation measurements.




TABLE IV  
CALCULATED ATTENUATION COEFFICIENTS FOR ULTIMATE LAYER BURNOUT

Element	Mass Absorption Coeff - cm <sup>2</sup> /gm		Residue Composition gm/cm		Attenuation Coefficients, cm <sup>-1</sup>			
	neutron	gamma	Test*	Expected**	Neutrons		Gamma	
					Test	Expected	Test	Expected
H	0.91	0.0445	0.0030	0	0.0027	0	0.0001	0
C	0.040	0.0244	0.0240	0.1035	0.0010	0.0041	0.0006	0.0025
O	0.036	0.0253	0.0215	0	0.0008	0	0.0005	0
Fe	0.021	0.0312	3.568	3.568	0.0749	0.0749	0.1113	0.1113
Totals	---	---	3.617	3.672	0.0794	0.0790	0.1125	0.1138

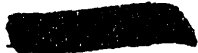
\* The amount of masonite which was used in the test to approximate the ultimate burnout of a given layer was a 5/16" thick layer of masonite, or approximately 7% of the original content of carbon, hydrogen and oxygen. This is noted in the table above as "test" residue.

\*\* The ultimate residue remaining after heating masonite consists of approximately 30% of the original carbon content and none of the original hydrogen and oxygen content. This is noted in the table above as "expected" residue.

From the results of the calculations in Table IV it can be concluded that the second set of test configurations (3A, 4A) was a suitable substitute for the anticipated residue for both fast neutrons and photons. The presence of the small amount of hydrogen remaining in the masonite used in the test shield might perturb the relationship that would actually exist for the intermediate energy neutrons. A calculation was made by L. A. Wilson comparing the test residue and the expected residue on the basis of slowing-down powers which indicated the two cases to be equivalent; nonetheless an unknown, though probably small, uncertainty is introduced because of the use of masonite rather than carbon as the residue material.

#### 4. Capture Gamma Flux

The gamma measurements (see Figure 13) indicate an anomalously high point for the worst burnout case, 4A. It is felt that this might be explained by the presence of capture gamma radiation, but a rigorous proof has not been made. If the cadmium covered gold activity in the outer layer of iron is plotted along with the gamma data as a function of masonite removed, it is found that a similar shaped curve is formed, although the foil activity did not exhibit as much of an increase in neutron level between configuration 4 and 4A as that observed for gamma activity. Because of the large jump in the gamma intensity which was found in going from 4 to 4A, it is possible that even larger increases could occur for worse cases of burnout. This would be undesirable because the high energy photons which result from thermal neutron capture in iron are more difficult to shield than are the intermediate energy neutrons which are the predominate source of the biological dose rate at stage 4A of burnout. Some doubt exists as to the correct method of extrapolating gamma intensity to the maximum degree of burnout, but it is concluded that additional gamma shielding would probably be required for this situation.




## 5. Temperature Distribution

Several shield temperature distribution measurements have been taken in the C test hole at the H pile and in the DR shield test facilities, which have shown a linear temperature drop from the thermal shield to the outside skin of the biological shield (neglecting laminar effects). This is the condition which would be expected to exist if (1) the sources of heat within the biological shield were small compared to the heat flowing from the thermal shield through the biological shield and/or if (2) the thermal conductivity of the gross biological shield structure were uniform over each of the laminar cycles. It was noted during the test that as the shield was altered by removing sheets of masonite from a slab the temperature distribution changed so that more slabs were approaching the temperature of the thermal shield (or in this case of the flange of the T section.) Representative shield temperature traverses shown in Figure 14 illustrate this observation. Because of the exponential decrease in heat generation rate it seems unlikely that condition (1) above can be altered; therefore, the altered temperature distribution is attributed to the air gaps being better conductors of heat than were the original layers of masonite. Under these circumstances the burnout rate of each succeeding layer would be accelerated rather than retarded by the burnout of the previous layer. The uncertainty created by this point makes the time rate of burnout of the layers much more difficult to take into account in predicting shield conditions. This uncertainty does not enter into the present experiment but does affect the accuracy of the curves presented in references 1 and 2.

## 6. Facility Edge Effects


Bulk shield measurements are subject to edge effects created not only because of the clearance allowed between the test slabs and the test well but also because the material under test does not possess the same attenuation characteristics as the surrounding shield material. In



previous tests the streaming through the clearance caused an increase in the readings within the test slabs. The effect was usually small and a correction was made when necessary; if not corrected the effect made the results conservatively high. In the present test the attenuating properties of the burned out layers are so poor that there is streaming from the test well out into the shield in spite of the clearance between the well and the slabs. As before, the correction does not appear to be large but in the present case the lack of correction would tend to leave the measurements on the nonconservative side.

#### D. Conclusions

Although the measurements contain uncertainties which might minimize their value in basic shielding work, the tests are sufficiently valid for predicting leakage through severely burned out shields to indicate the scope of the problem. For example, under severe burnout conditions radiation leakage will become sufficient to prevent access to certain regions of the pile building; neutrons will become the dominant component of the radiation leakage as the shield deteriorates. Because of this information, current experimental work is being directed toward precluding serious limitations to pile life and operating efficiency due to shield radiation leakage. Work in progress includes a study of the use of fringe poison to reduce shield temperatures and thus extend the life expectancy of the masonite and a search for better neutron detecting devices which would more accurately define the dose rate.



ACKNOWLEDGMENTS

A substantial portion of the work covered by this report was performed by R. L. Tomlinson and L. A. Wilson who are no longer associated with the Hanford shielding program; the foil activation data were obtained by Tomlinson and the masonite deterioration studies were carried out by Wilson.

*W. L. Bunch*


---

W. L. Bunch

WLB:ms



REFERENCES

- (1) HW-38419, "Iron-Masonite Shield Effectiveness as a Function of Pile Operating Conditions", L. A. Wilson, 9-19-55 (Secret).
  - (2) HW-35202, "Hanford Shield Masonite Deterioration Studies", L. A. Wilson, 8-8-55 (Secret).
  - (3) HW-40997, "Interim Report - PT-105-604-A Reducing Side Shield Temperature by Fringe Poisoning", W. L. Bunch, 1-19-56 (Secret).
  - (4) HW-41189, "FY 1958 Budget Study, Shield Patches, B, D, F, DR, and H Reactors", C. A. Mansius, 2-1-56 (Official Use Only).
  - (5) HW-41507, "Possible Mechanical Effects of Extreme Masonite Deterioration in Laminated Biological Shields", G. J. Rogers, 3-22-56 (SECRET).
  - (6) HW-36370, "Attenuation Properties of Hanford Pile Shield Materials", W. L. Bunch and R. L. Tomlinson, 9-1-55 (Secret).
  - (7) HW-26207, "The Standardization of Gold and Indium Foils and the Absolute Neutron Flux Determination in the Hanford Standard Pile", D. E. Davenport, G. L. Lynn, and C. R. Richey, 8-27-54 (Declassified).
  - (8) HW-29125, "Measurement of Neutron Fluxes in Graphite Reflector", R. L. Tomlinson, 9-1-53 (Secret).
  - (9) HW-29135, "Measurement of Neutron Flux Spectra Inside Reactors", R. E. Heineman, 8-26-53 (Secret).
  - (10) HW-28303, "Neutron Energy Spectra in a Hanford Pile", R. E. Heineman, and J. W. Culvahouse, 6-5-53 (Secret).
  - (11) RH-1 Reactor Handbook, Volume 1, June 1955, page 946 (Secret).
  - (12) BNL-351, "Neutron Monitoring with Indium Foils", F. B. Oleson, July 1955.
  - (13) Physical Review, Volume 85, No. 4, February 15, 1952, "Neutron Transmission Cross Sections in the Kilovolt Region", Carl T. Hibdon, Alexander Langsdorf, Jr., and Robert E. Holland.
  - (14) Personal Communication, Henry W. Newson, to be published in Physical Review, Volume 102, No. 6, June 15, 1956.
- 

APPENDIX

The Appendix consists of a set of tables containing foil activation data from the various burnout configurations. Each tabulated point in Table V through Table X represents the "best" central point activity and is a result of the analysis of the several foils placed in the form of a cross at each depth of penetration. Bare gold foils were irradiated at each depth but cadmium covered gold and sulfur foils were placed only within the iron layers. For this reason the measured cadmium ratios are low, indicating the absorption of the thermal neutrons in the iron. The foil activities are normalized to the power level of the pile and are given in terms of counts per minute per gram per 100 megawatts.

Table XI contains the saturated activity of all of the foil data obtained in the paraffin and lucite integrators. These are also normalized to pile power level and are given in counts per minute per gram per 100 megawatts. No correction has been applied to these data for the helical pattern in which they were loaded.






TABLE V

BURNOUT CONFIGURATION 1SATURATED ACTIVITY OF FOILS

Actual Distance from Reflector (inches)	Effective Distance from Reflector (inches)	Activity - Counts / minute · gram · 100 MW		
		Bare Gold	Cadmium Covered Gold	Cadmium Covered Sulfur
16.38	13.75	$9.8 \times 10^7$	$8.4 \times 10^7$	
17.63	15	$7.4 \times 10^7$	$5.8 \times 10^7$	$4.80 \times 10^3$
19	16.38	$9.6 \times 10^7$		
20.13	17.50	$1.30 \times 10^8$		
21.13	18.50	$8.4 \times 10^7$		
24.63	19.75	$1.48 \times 10^7$	$1.08 \times 10^7$	
25.88	21	$7.7 \times 10^6$	$5.6 \times 10^6$	$4.27 \times 10^2$
27.25	22.38	$6.8 \times 10^6$		
28.38	23.50	$9.4 \times 10^6$		
29.38	24.50	$7.7 \times 10^6$		
30.38	25.50	$4.3 \times 10^6$		
32.88	26.88	$5.5 \times 10^5$	$2.6 \times 10^5$	
34.13	28.13	$2.4 \times 10^5$	$1.78 \times 10^5$	31.6
35.50	29.50	$1.7 \times 10^5$		
36.63	30.63	$2.3 \times 10^5$		
37.63	31.63	$1.85 \times 10^5$		
38.63	32.63	$1.15 \times 10^5$		
39.75	33.75	$5.3 \times 10^4$		
41.13	35.13	$6.7 \times 10^3$	$2.45 \times 10^3$	
42.38	36.38	$2.45 \times 10^3$	$1.40 \times 10^3$	3.06

TABLE V (contd.)

<u>Actual Distance from Reflector (inches)</u>	<u>Effective Distance from Reflector (inches)</u>	<u>Activity - Counts/minute · gram · 100 MW</u>		
		<u>Bare Gold</u>	<u>Cadmium Covered Gold</u>	<u>Cadmium Covered Sulfur</u>
43.75	37.75	$2.2 \times 10^3$		
44.88	38.88	$3.3 \times 10^3$		
45.88	39.88	$2.9 \times 10^3$		
46.88	40.88	$1.95 \times 10^3$		
48.25	42.25	$6.8 \times 10^2$		
49.38	43.38	$9.0 \times 10$	$4.50 \times 10$	
50.63	44.63	$4.1 \times 10$	$3.25 \times 10$	
52	46	$6.6 \times 10$		
53.13	47.13	$8.8 \times 10$		
54.13	48.13	$7.2 \times 10$		
55.13	49.13	$5.3 \times 10$		
56.25	50.25	$1.75 \times 10$		
57.63	51.63	4.0	6.3	
58.88	52.88	5.3	8.2	

TABLE VI

BURNOUT CONFIGURATION 2SATURATED ACTIVITY OF FOILS

Actual Distance from Reflector (inches)	Effective Distance from Reflector (inches)	Activity - Counts/minute · gram · 100 MW		
		Bare Gold	Cadmium Covered Gold	Cadmium Covered Sulfur
11.63	11.63	$3.15 \times 10^8$		
16.38	13.75	$1.32 \times 10^8$	$1.18 \times 10^8$	
17.63	15	$9.4 \times 10^7$	$7.8 \times 10^7$	$5.026 \times 10^3$
19	16.38	$1.25 \times 10^8$		
24.63	18.63	$2.25 \times 10^7$	$2.18 \times 10^7$	
25.88	19.88	$1.62 \times 10^7$	$1.34 \times 10^7$	$5.67 \times 10^2$
27.25	21.25	$1.35 \times 10^7$		
28.38	22.38	$1.80 \times 10^7$		
29.38	23.38	$1.15 \times 10^7$		
32.88	24.63	$1.82 \times 10^6$	$1.14 \times 10^6$	
34.13	25.88	$8.5 \times 10^5$	$6.4 \times 10^5$	48.54
35.50	27.25	$6.8 \times 10^5$		
36.63	28.38	$9.9 \times 10^5$		
37.63	29.38	$8.0 \times 10^5$		
38.63	30.38	$4.3 \times 10^5$		
41.13	31.75	$5.1 \times 10^4$	$2.55 \times 10^4$	
42.38	33	$2.25 \times 10^4$	$1.65 \times 10^4$	4.49
43.75	34.38	$2.2 \times 10^4$		
44.88	35.50	$2.9 \times 10^4$		
45.88	36.50	$2.41 \times 10^4$		
46.88	37.50	$1.67 \times 10^4$		

TABLE VI (contd.)

Actual Distance from Reflector (inches)	Effective Distance from Reflector (inches)	Activity - Counts/minute · gram · 100 MW		
		Bare Gold	Cadmium Covered Gold	Cadmium Covered Sulfur
48.25	38.88	$6.1 \times 10^3$		
49.38	40	$7.3 \times 10^2$	$3.7 \times 10^2$	
50.63	41.25	$2.75 \times 10^2$	$1.60 \times 10^2$	
52	42.63	$5.8 \times 10^2$		
53.13	43.75	$8.3 \times 10^2$		
54.13	44.75	$5.8 \times 10^2$		
55.13	45.75	$4.8 \times 10^2$		
56.25	46.88	$1.43 \times 10^2$		
57.63	48.25	$6.9 \times 10$	$1.45 \times 10$	
58.88	49.50	$1.85 \times 10$	$1.0 \times 10$	

TABLE VII

BURNOUT CONFIGURATION 3SATURATED ACTIVITY OF FOILS

<u>Actual Distance from Reflector (inches)</u>	<u>Effective Distance from Reflector (inches)</u>	Activity - Counts/minute · gram · 100 MW		
		<u>Bare Gold</u>	<u>Cadmium Covered Gold</u>	<u>Cadmium Covered Sulfur</u>
11.63	11.63	$3.15 \times 10^8$		
16.38	13.75	$1.34 \times 10^8$	$1.13 \times 10^8$	
17.63	15	$8.82 \times 10^7$	$7.64 \times 10^7$	$4.99 \times 10^3$
19	16.38	$1.17 \times 10^8$		
24.63	18.63	$2.84 \times 10^7$	$2.21 \times 10^7$	
25.88	19.88	$1.68 \times 10^7$	$1.40 \times 10^7$	$5.46 \times 10^2$
27.25	21.25	$1.67 \times 10^7$		
32.88	23.50	$3.91 \times 10^6$	$3.30 \times 10^6$	
34.13	24.75	$2.20 \times 10^6$	$1.79 \times 10^6$	84.9
35.50	26.13	$2.35 \times 10^6$		
36.63	27.25	$3.59 \times 10^6$		
37.63	28.25	$2.78 \times 10^6$		
41.13	29.50	$3.24 \times 10^5$	$1.54 \times 10^5$	
42.38	30.75	$1.46 \times 10^5$	$9.69 \times 10^4$	10
43.75	32.13	$1.72 \times 10^5$		
44.88	33.25	$1.45 \times 10^5$		
45.88	34.25	$7.45 \times 10^4$		
46.88	35.25	$9.0 \times 10^3$		
49.38	36.63	$3.75 \times 10^3$	$2.74 \times 10^3$	
50.63	37.88	$3.40 \times 10^3$	$2.22 \times 10^3$	
52	39.25	$4.20 \times 10^3$		
53.13	40.38	$4.90 \times 10^3$		

TABLE VII (contd.)

<u>Actual Distance from Reflector (inches)</u>	<u>Effective Distance from Reflector (inches)</u>	<u>Activity - Counts/minute · gram · 100 MW</u>		
		<u>Bare Gold</u>	<u>Cadmium Covered Gold</u>	<u>Cadmium Covered Sulfur</u>
54.13	41.38	$4.20 \times 10^3$		
55.13	42.38	$2.52 \times 10^3$		
56.25	43.50	$7.9 \times 10^2$		
57.63	44.88	$9.10 \times 10$	$2.90 \times 10$	
58.88	46.13	$5.7 \times 10$	$1.52 \times 10$	

TABLE VIIIBURNOUT CONFIGURATION 4SATURATED ACTIVITY OF FOILS

Actual Distance from Reflector (inches)	Effective Distance from Reflector (inches)	Activity - Counts/minute · gram · 100 MW		
		Bare Gold	Cadmium Covered Gold	Cadmium Covered Sulfur
11.63	11.63	$3.15 \times 10^8$		
16.38	13.75	$1.37 \times 10^8$	$1.14 \times 10^8$	
17.63	15	$7.82 \times 10^7$	$5.00 \times 10^7$	$5.00 \times 10^3$
19	16.38	$1.12 \times 10^8$		
19.75	17.13	$1.17 \times 10^8$		
24.63	18.63	$2.25 \times 10^7$	$1.82 \times 10^7$	
25.88	19.88	$1.39 \times 10^7$	$1.28 \times 10^7$	$5.19 \times 10^2$
27.25	21.25	$1.50 \times 10^7$		
28	22	$1.39 \times 10^7$		
32.88	23.50	$3.31 \times 10^6$	$2.58 \times 10^6$	
34.13	24.75	$1.48 \times 10^6$	$1.06 \times 10^6$	$7.11 \times 10^1$
35.50	26.13	$1.85 \times 10^6$		
36.25	26.88	$1.76 \times 10^6$		
41.13	28.38	$4.29 \times 10^5$	$2.93 \times 10^5$	
42.38	29.63	$2.39 \times 10^5$	$1.79 \times 10^5$	7.85
43.75	30	$2.39 \times 10^5$		
44.88	32.13	$2.77 \times 10^5$		
45.50	32.75	$1.79 \times 10^5$		
49.38	34.38	$3.75 \times 10^4$	$2.23 \times 10^4$	
50.63	35.63	$1.82 \times 10^4$	$1.15 \times 10^4$	0.96
52	37	$2.61 \times 10^4$		
53.13	38.13	$1.96 \times 10^4$		

## UNCLASSIFIED

-46-

HW-38418

TABLE VIII (contd.)

Actual Distance from Reflector (inches)	Effective Distance from Reflector (inches)	Activity - Counts/minute · gram · 100 MW		
		Bare Gold	Cadmium Covered Gold	Cadmium Covered Sulfur
54.13	39.13	$1.96 \times 10^4$		
54.88	39.88	$1.03 \times 10^4$		
57.63	41.50	$1.16 \times 10^3$	$4.29 \times 10^2$	
58.88	42.75	$7.28 \times 10^2$	$1.73 \times 10^2$	



TABLE IX  
BURNOUT CONFIGURATION 3A  
SATURATED ACTIVITY OF FOILS

<u>Actual Distance from Reflector (inches)</u>	<u>Effective Distance from Reflector (inches)</u>	<u>Activity - Counts/minute · gram · 100 MW</u>		
		<u>Bare Gold</u>	<u>Cadmium Covered Gold</u>	<u>Cadmium Covered Sulfur</u>
11.63	11.63	$2.45 \times 10^8$		
16.38	13	$1.38 \times 10^8$	$1.20 \times 10^8$	
17.63	14.25	$1.03 \times 10^8$	$9.3 \times 10^7$	$1.18 \times 10^4$
18.88	15.50	$9.00 \times 10^7$		
24.63	17.06	$5.20 \times 10^7$	$4.4 \times 10^7$	
25.88	18.31	$3.70 \times 10^7$	$3.60 \times 10^7$	$2.35 \times 10^3$
27.13	19.56	$6.40 \times 10^7$		
28	20.44	$4.00 \times 10^7$		
32.88	22.13	$1.48 \times 10^7$	$1.08 \times 10^7$	
34.13	23.38	$7.50 \times 10^6$	$6.22 \times 10^6$	$2.35 \times 10^2$
35.38	24.63	$9.80 \times 10^6$		
36.38	25.63	$1.20 \times 10^7$		
37.31	26.56	$9.20 \times 10^6$		
41.13	28.25	$9.70 \times 10^5$	$7.6 \times 10^5$	
42.38	29.50	---	$4.6 \times 10^5$	$1.72 \times 10^1$
43.63	30.75	$5.30 \times 10^5$		
44.63	31.75	$6.20 \times 10^5$		
45.63	32.75	$6.20 \times 10^5$		
46.69	33.81	$2.90 \times 10^5$		
49.38	35.50	$3.05 \times 10^4$	$1.20 \times 10^4$	

TABLE IX (contd.)

<u>Actual Distance from Reflector (inches)</u>	<u>Effective Distance from Reflector (inches)</u>	<u>Activity - Counts/minute · gram · 100 MW</u>		
		<u>Bare Gold</u>	<u>Cadmium Covered Gold</u>	<u>Cadmium Covered Sulfur</u>
50.63	36.75	$1.30 \times 10^4$	$7.30 \times 10^3$	
51.88	38	$1.04 \times 10^4$		
52.88	39	$1.40 \times 10^4$		
53.88	40	$1.18 \times 10^4$		
54.88	41	$6.50 \times 10^3$		
55.75	41.88	$3.30 \times 10^3$		
57.63	43.50	$3.00 \times 10^2$	$8.4 \times 10^1$	
58.88	44.75	$1.40 \times 10^2$	$4.5 \times 10^1$	

TABLE X

BURNOUT CONFIGURATION 4ASATURATED ACTIVITY OF FOILS

Actual Distance from Reflector (inches)	Effective Distance from Reflector (inches)	Activity - Counts/minute · gram · 100 MW		
		Bare Gold	Cadmium Covered Gold	Cadmium Covered Sulfur
11.75	11.75	$2.30 \times 10^8$		
16.38	13	$1.31 \times 10^8$	$1.19 \times 10^8$	
17.63	14.25	$9.44 \times 10^7$	$8.62 \times 10^7$	
18.88	15.50	$8.88 \times 10^7$		
24.63	17.06	$5.13 \times 10^7$	$5.08 \times 10^7$	
25.88	18.31	$4.61 \times 10^7$	$3.49 \times 10^7$	$2.00 \times 10^3$
27.13	19.56	$3.49 \times 10^7$		
32.88	21.13	$2.06 \times 10^7$	$1.70 \times 10^7$	
34.13	22.38	$1.50 \times 10^7$	$1.25 \times 10^7$	$3.06 \times 10^2$
35.88	23.63	$2.84 \times 10^7$		
36.06	24.31	$1.83 \times 10^7$		
41.13	25.69	$6.71 \times 10^6$	$4.11 \times 10^6$	
42.38	26.94	$3.91 \times 10^6$	$3.20 \times 10^6$	38.7
43.63	28.19	$7.34 \times 10^6$		
44.63	29.19	$8.96 \times 10^6$		
45.56	30.13	$4.82 \times 10^6$		
45.88	30.44	$2.74 \times 10^6$		
49.38	31.81	$5.87 \times 10^5$	$3.30 \times 10^5$	
50.63	33.06	$2.44 \times 10^5$	$1.95 \times 10^5$	
51.88	34.31	$2.39 \times 10^5$		
52.88	35.31	$3.34 \times 10^5$		

UNCLASSIFIED

TABLE X (contd.)

<u>Actual Distance from Reflector (inches)</u>	<u>Effective Distance from Reflector (inches)</u>	<u>Activity - Counts/minute · gram · 100 MW</u>		
		<u>Bare Gold</u>	<u>Cadmium Covered Gold</u>	<u>Cadmium Covered Sulfur</u>
53.88	36.31	$2.67 \times 10^5$		
54.88	37.31	$1.54 \times 10^5$		
57.63	39.56	$9.27 \times 10^3$	$2.81 \times 10^3$	
58.88	40.81	$4.06 \times 10^3$	$1.11 \times 10^3$	

TABLE XI  
FOIL ACTIVATION DATA, INTEGRATOR SUMMARY

PARAFFIN		LUCITE											
CONF. 1		CONF. 2		CONF. 3		CONF. 4		CONF. 4A		CONF. 4		CONF. 4	
Dist. Inches	Bare* Gold	Dist. Inches	Bare* Gold	Dist. Inches	Bare* Gold	Dist. Inches	Bare* Gold	Dist. Inches	Bare* Gold	Dist. Inches	Bare* Gold	Dist. Inches	Cadmium* Covered Gold
0	1.44	0	17.2	0	20.1	0	5.58 x 10 <sup>2</sup>	0	3.46 x 10 <sup>3</sup>	0	3.46 x 10 <sup>3</sup>	0	37.3
1.5	0.83	1.5	21.0	0.500	31.4	0.375	7.4 x 10 <sup>2</sup>	0.437	4.53 x 10 <sup>3</sup>	0.437	4.53 x 10 <sup>3</sup>	0.437	39.3
3.0	0.63	3.0	11.6	1.000	34.4	0.750	8.09 x 10 <sup>2</sup>	0.875	4.64 x 10 <sup>3</sup>	0.875	4.64 x 10 <sup>3</sup>	0.875	29.7
4.5	1.11	4.5	7.4	1.500	36.0	1.125	7.49 x 10 <sup>2</sup>	1.312	4.64 x 10 <sup>3</sup>	1.312	4.64 x 10 <sup>3</sup>	1.312	16.0
6.0	1.09	6.0	2.1	2.000	33.3	1.500	6.8 x 10 <sup>2</sup>	1.750	4.17 x 10 <sup>3</sup>	1.750	4.17 x 10 <sup>3</sup>	1.750	11.6
				2.500	28.1	1.875	6.21 x 10 <sup>2</sup>	2.187	3.42 x 10 <sup>3</sup>	2.187	3.42 x 10 <sup>3</sup>	2.187	10.1
				3.000	26.1	2.250	5.36 x 10 <sup>2</sup>	2.625	2.71 x 10 <sup>3</sup>	2.625	2.71 x 10 <sup>3</sup>	2.625	6.06
				3.500	19.7	2.625	4.49 x 10 <sup>2</sup>	3.063	2.02 x 10 <sup>3</sup>	3.063	2.02 x 10 <sup>3</sup>	3.063	3.12
				4.000	18.0	3.000	3.53 x 10 <sup>2</sup>	3.500	1.48 x 10 <sup>3</sup>	3.500	1.48 x 10 <sup>3</sup>	3.500	2.91
				4.500	15.4	3.375	3.00 x 10 <sup>2</sup>	3.937	1.17 x 10 <sup>3</sup>	3.937	1.17 x 10 <sup>3</sup>	3.937	2.02
				5.000	13.1	3.750	2.43 x 10 <sup>2</sup>	4.375	8.41 x 10 <sup>2</sup>	4.375	8.41 x 10 <sup>2</sup>	4.375	0.99
				5.500	10.2	4.125	1.79 x 10 <sup>2</sup>	4.813	6.68 x 10 <sup>2</sup>	4.813	6.68 x 10 <sup>2</sup>	4.812	0.97
				6.000	9.0	4.500	1.38 x 10 <sup>2</sup>	5.250	5.08 x 10 <sup>2</sup>	5.250	5.08 x 10 <sup>2</sup>	5.250	1.42
				6.500	7.9	4.875	1.08 x 10 <sup>2</sup>	5.687	3.46 x 10 <sup>2</sup>	5.687	3.46 x 10 <sup>2</sup>	5.687	1.13
				5.250	5.9	5.250	7.76 x 10 <sup>1</sup>	6.125	2.47 x 10 <sup>2</sup>	6.125	2.47 x 10 <sup>2</sup>	6.125	
				5.625	5.1	5.625	5.95 x 10 <sup>1</sup>	6.562	1.66 x 10 <sup>2</sup>	6.562	1.66 x 10 <sup>2</sup>	6.562	
				6.000		6.000	5.33 x 10 <sup>1</sup>	7.000	1.19 x 10 <sup>2</sup>	7.000	1.19 x 10 <sup>2</sup>	7.000	
				6.375		6.375	4.57 x 10 <sup>1</sup>	7.437	9.05 x 10 <sup>1</sup>	7.437	9.05 x 10 <sup>1</sup>	7.437	
				6.750		6.750	3.24 x 10 <sup>1</sup>	7.875	6.76 x 10 <sup>1</sup>	7.875	6.76 x 10 <sup>1</sup>	7.875	
				7.125		7.125	2.42 x 10 <sup>1</sup>	8.313	6.53 x 10 <sup>1</sup>	8.313	6.53 x 10 <sup>1</sup>	8.313	
				7.500		7.500	2.58 x 10 <sup>1</sup>	8.750	5.04 x 10 <sup>1</sup>	8.750	5.04 x 10 <sup>1</sup>	8.750	
				7.875		7.875	1.53 x 10 <sup>1</sup>	9.187	2.76 x 10 <sup>1</sup>	9.187	2.76 x 10 <sup>1</sup>	9.187	
				8.250		8.250	1.14 x 10 <sup>1</sup>	9.625	1.90 x 10 <sup>1</sup>	9.625	1.90 x 10 <sup>1</sup>	9.625	
				8.625		8.625	9.49	10.063	1.64 x 10 <sup>1</sup>	10.063	1.64 x 10 <sup>1</sup>	10.063	
				9.000		9.000	9.51	10.500	8.75	10.500	8.75	10.500	
				9.375		9.375	9.56	10.937	5.64	10.937	5.64	10.937	
				9.750		9.750	5.82	11.375	4.26	11.375	4.26	11.375	
				10.125		10.125	5.89						
				10.500		10.500	5.85						
				10.875		10.875	3.78						

\* All foil activities are in counts/minute · gram · 100 MW.

UNCLASSIFIED

- 52 -

HW-38418

ABSTRACT

Following experimental studies which had showed that thermal effects are predominant in the deterioration of the masonite in the older Hanford pile shields, a series of radiation attenuation measurements were carried out in the DR test wells in which progressive burnout stages were simulated by voids. Results of these experimental measurements are presented for use in determining future radiation leakage problems and their resolution.

**END**

---

**DATE  
FILMED**

5/25/93

